

UNCLASSIFIED

AD NUMBER

ADB011996

LIMITATION CHANGES

TO:

Approved for public release; distribution is unlimited.

FROM:

Distribution authorized to U.S. Gov't. agencies only; Test and Evaluation; OCT 1975. Other requests shall be referred to Air Force Wright Aeronautical Labs., Wright-Patterson AFB, OH.

AUTHORITY

AFFDL ltr 27 Dec 1977

THIS PAGE IS UNCLASSIFIED

THIS REPORT HAS BEEN DELIMITED  
AND CLEARED FOR PUBLIC RELEASE  
UNDER DOD DIRECTIVE 5200.20 AND  
NO RESTRICTIONS ARE IMPOSED UPON  
ITS USE AND DISCLOSURE.

DISTRIBUTION STATEMENT A

APPROVED FOR PUBLIC RELEASE;  
DISTRIBUTION UNLIMITED.

*P*

AD B O I 1996

# A NEW FINITE ELEMENT SUPERSONIC KERNEL FUNCTION METHOD IN LIFTING SURFACE THEORY

FINAL REPORT

LOCKHEED MISSILES & SPACE COMPANY, INC.  
HUNTSVILLE RESEARCH & ENGINEERING CENTER  
4800 BRADFORD DRIVE, HUNTSVILLE, AL 35807

DDC  
RECEIVED  
JUL 6 1976  
HUNTSVILLE

APRIL 1976

REPORT FOR PERIOD 20 OCTOBER 1974 - 20 OCTOBER 1975

AD No. \_\_\_\_\_  
DDC FILE COPY

Distribution limited to U.S. Government agencies only; test and evaluation statement applied October 1975. Other requests for this document must be referred to AF Flight Dynamics Laboratory (FBR), Wright-Patterson Air Force Base, Ohio 45433.

AIR FORCE FLIGHT DYNAMICS LABORATORY  
AIR FORCE WRIGHT AERONAUTICAL LABORATORIES  
Air Force Systems Command  
Wright-Patterson Air Force Base, Ohio 45433

NOTICE

When Government drawings, specifications, or other data are used for any purpose other than in connection with a definitely related Government procurement operation, the United States Government thereby incurs no responsibility nor any obligation whatsoever; and the fact that the government may have formulated, furnished, or in any way supplied the said drawings, specifications, or other data, is not to be regarded by implication or otherwise in any manner licensing the holder or any other person or corporation, or conveying any rights or permission to manufacture, use, or sell any patented invention that may in any way be related thereto.

This technical report has been reviewed and is approved for publication.

*Gerald M. Van Keuren*

GERALD M. VAN KEUREN, CAPTAIN, USAF  
Project Engineer  
Optimization Group  
Analysis and Optimization Branch

FOR THE COMMANDER

*Gerald G. Leigh*

GERALD G. LEIGH, Lt. Col, USAF  
Chief, Structures Division

ADDITIONAL BY	
RTIS	<input checked="" type="checkbox"/>
GDD	<input checked="" type="checkbox"/>
ENA - UNCLASSIFIED	<input type="checkbox"/>
JOURNALS	
BY	
DISTRIBUTION AVAILABILITY CODES	
Dist. Avail. Code	
<b>B</b>	

Copies of this report should not be returned unless return is required by security considerations, contractual obligations, or notice on a specific document.

AIR FORCE - 21 JUNE 76 - 100



## FOREWORD

This report was prepared by personnel in the Engineering Sciences Section of the Lockheed Missiles & Space Company, Inc., Huntsville Research & Engineering Center, Huntsville, Alabama, for the Air Force Flight Dynamics Laboratory, Wright-Patterson Air Force Base, Ohio. The research study was performed under Project 1370, "Dynamic Problems in Flight Vehicles," Task 137004, "Design Analysis," Contract F33615-75-C-3001. Capt. Gerald Van Keuren, AFFDL/FBR, was the Air Force Project Engineer.

V. Y. C. Young was the principal investigator under the supervision of M. R. Brashears.

The user's manual for the computer program developed in this study is documented as AFFDL-TR-76-3, Vol. II.

## TABLE OF CONTENTS

<u>Section</u>		<u>Page</u>
I	INTRODUCTION	1
II	FORMULATION	2
	2.1 Small Perturbation Formulation	2
	2.2 Acceleration Potential	5
	2.3 Integral Equation Approach	6
III	EXISTING METHODS	9
	3.1 Integrated Downwash Method	9
	3.2 Kernel Function Method	12
	3.3 Integrated Potential Method	15
	3.4 General Theory of Unsteady Compressible Potential Aerodynamics	16
	3.5 Recommendations	17
IV	PRESENT METHOD	
	4.1 Theoretical Considerations	18
	4.2 Statement of the Problem	19
	4.3 Finite Element Formulation	22
	4.4 Choice of Elements	24
	4.5 Choice of Mesh	25
	4.6 Finite Element Integration Scheme	26
	4.7 Integration Across the Singular Strip	28
	4.8 Starting Solution	30
	4.9 Edge Conditions and Gaussian Quadrature	32
	4.10 Kernel Function Evaluation	35
	4.11 Solution Procedure	36
V	RESULTS AND DISCUSSION	37
	REFERENCES	88

## LIST OF TABLES

<u>Table</u>		<u>Page</u>
1	Comparison of the Two Versions of Kernel Subroutine	45
2	Summary of Demonstration Cases	46
3	Computer Program Statistics for Rectangular A = 2	47
4	Computer Program Statistics for Arrowhead A = 4	48
5	Computer Program Statistics for Tapered Sweptback A = 1.45	49
6-13	$Q_{ij}$ in AGARD Notation, Aspect Ratio 2.0 Rectangular	
6	M = 1.2, k = 0.0	51
7	M = 1.2, k = 0.3	52
8	M = 1.2, k = 0.6	53
9	M = 1.2, k = 1.0	54
10	M = 2.0, k = 0.0	56
11	M = 2.0, k = 0.3	57
12	M = 2.0, k = 0.6	58
13	M = 2.0, k = 1.0	59
14-25	$Q_{ij}$ in AGARD Notation, Aspect Ratio 4.0 Arrowhead Wing	
14	M = 1.12, k = 0.0	61
15	M = 1.12, k = 0.5	62
16	M = 1.12, k = 1.0	63
17	M = 1.25, k = 0.0	65
18	M = 1.25, k = 0.5	66
19	M = 1.25, k = 1.0	67
20	M = 1.5621, k = 0.0	69
21	M = 1.5621, k = 0.5	70
22	M = 1.5621, k = 1.0	71
23	M = 2.0, k = 0.0	73
24	M = 2.0, k = 0.5	74
25	M = 2.0, k = 1.0	75

LIST OF TABLES (Continued)

<u>Table</u>		<u>Page</u>
26-34	$Q_{ij}$ in AGARD Notation, Aspect Ratio 1.45 Tapered Swept-Back Wing	
26	M = 1.04, k = 0.0	77
27	M = 1.04, k = 0.5	78
28	M = 1.04, k = 1.0	79
29	M = 1.2, k = 0.0	81
30	M = 1.2, k = 0.5	82
31	M = 1.2, k = 1.0	83
32	M = 2.0, k = 0.0	85
33	M = 2.0, k = 0.5	86
34	M = 2.0, k = 1.0	87

LIST OF ILLUSTRATIONS

<u>Figure</u>		<u>Page</u>
1	Arbitrarily Aligned Mesh	39
2	Quadratic Elements vs Linear Elements	40
3	Nonuniform Mesh	41
4	Typical Elements Used to Fit the Planform	42
5	Regular Mesh with Irregular Elements at Planform Edges	43
6	Regions of Integration for Conventional Kernel Function Method	44
7	Regions of Integration for Present Method	44
8	Mesh Used for Rectangular A = 2.0, M = 1.2	50
9	Mesh Used for Rectangular A = 2.0, M = 2.0	55
10	Mesh Used for Arrowhead A = 4.0, M = 1.12	60
11	Mesh Used for Arrowhead A = 4.0, M = 1.25	64
12	Mesh Used for Arrowhead A = 4.0, M = 1.5621	68
13	Mesh Used for Arrowhead A = 4.0, M = 2.0	72
14	Mesh Used for Tapered Sweptback A = 1.45, M = 1.04	76
15	Mesh Used for Tapered Sweptback A = 1.45, M = 1.2	80
16	Mesh Used for Tapered Sweptback A = 1.45, M = 2.0	84

## LIST OF SYMBOLS

<u>Symbol</u>	
$C$	Region of integration bounded by forward Mach lines
$\bar{C}(e)$	weighted kernel coefficients
$C_p$	pressure coefficient
$c$	speed of sound
$f_i$	dimensionless modal functions
$i$	$\sqrt{-1}$
$K$	kernel function
$k$	reduced frequency, $\omega s/V$
$l$	lift
$M$	freestream Mach number
$\bar{N}$	shape functions
$Q_{ij}$	generalized force coefficients
$Q'_{ij}$	real part of generalized force coefficients in AGARD notation
$Q''_{ij}$	imaginary part of generalized force coefficients in AGARD notation
$q_i(t)$	dimensionless generalized coordinates
$s$	semispan
$t$	time
$u$	perturbation velocity in x-direction
$V$	freestream velocity
$v$	perturbation velocity in y-direction
$W_i$	weights of the quadrature
$w$	perturbation velocity in z-direction
$\bar{w}$	complex upwash
$w_i$	weights of the quadrature

LIST OF SYMBOLS (Concluded)

Symbol

$x$	nondimensional coordinate
$x_0$	running coordinate in $x$ -direction
$y$	nondimensional coordinate
$y_0$	running coordinate in $y$ -direction
$Z$	dimensional vertical displacement
$\bar{z}$	modal deflection
$z$	nondimensional coordinate

Greek

$\beta$	$\sqrt{M^2 - 1}$
$\gamma$	specific heat ratio
$\xi$	abscissas of the quadrature
$\eta$	running coordinate in $y$ -direction
$\lambda_i$	lift due to a unit displacement in the $i^{\text{th}}$ generalized coordinate
$\bar{\lambda}(e)$	nodal lift vector at element level
$\xi$	running coordinate in $x$ -direction
$\rho$	density
$\phi$	velocity potential
$\psi$	acceleration potential
$\omega$	circular frequency

## SECTION I INTRODUCTION

For aeroelastic analysis, the aerodynamic forces are determined from the lifting surface theory. In the subsonic regime, the theory is well established. Most of the approaches are based on the kernel function method or a discretized variant called the doublet lattice method. In contrast, the supersonic lifting theory is still under active development and is further complicated by the fact that there is a variety of possible methods.

This study is directed toward the development of an accurate, efficient, inexpensive numerical procedure for the solution of the unsteady pressures on a planar wing undergoing simple harmonic oscillation in supersonic flow. An assessment on the theoretical and numerical aspects of several existing methods was made. It was concluded that all existing methods suffer some form of drawback.

Accordingly, an approach, which fully utilizes the merits of several of the various methods while collectively removing their respective disadvantages, is proposed. The method is based on a finite element approach to the supersonic kernel function method. It differs from the supersonic doublet lattice method in the following aspects. Instead of trapezoidal elements, characteristic elements are used. A linear element approximation on the lift is used instead of the constant doublet strength. Finally, the collocation point is consistently chosen to be at the nodes.

The new method offers a unified theory for both the subsonic and supersonic flow. It is also extendable to the transonic regime as well as to non-planar applications.

## SECTION II FORMULATION

### 2.1 Small Perturbation Formulation

For a thin wing traveling at a uniform velocity,  $V$ , the velocity field relative to the Cartesian coordinates fixed to the wing is given as

$$\begin{aligned}V_x &= V + u(x, y, z, t) \\V_y &= 0 + v(x, y, z, t) \\V_z &= 0 + w(x, y, z, t)\end{aligned}$$

where  $u, v$  and  $w$  are the perturbation velocities and satisfy the condition

$$u/V, v/V, w/V \ll 1$$

Assuming the flow field to be irrotational, a perturbation velocity potential,  $\phi$ , can be defined such that

$$u = \frac{\partial \phi}{\partial x}, \quad v = \frac{\partial \phi}{\partial y}, \quad w = \frac{\partial \phi}{\partial z}$$

According to the small perturbation theory, the perturbation velocity potential,  $\phi$ , for the subsonic, transonic and supersonic unsteady flow is governed by the following general differential equation

$$\left[ 1 - M^2 - \frac{M^2(\gamma+1)}{V} \phi_x \right] \phi_{xx} + \phi_{yy} + \phi_{zz} = \frac{1}{c^2} (2V \phi_{xt} + \phi_{tt}) \quad (1)$$

where  $M$  is the freestream Mach number;  $\gamma$ , the specific heat ratio of the fluid;  $V$ , the freestream velocity; and  $c$ , the speed of sound. Subscripts for  $\phi$  denote differentiation.

This equation can be further linearized for subsonic or supersonic flow (but not for transonic flow) to

$$(1 - M^2) \phi_{xx} + \phi_{yy} + \phi_{zz} = \frac{1}{c^2} (2 V \phi_{xt} + \phi_{tt}) \quad (2)$$

Despite the similarity in form, the differential equation assumes quite a different character depending on the freestream Mach number,  $M$ . For  $M < 1$ , the differential equation is elliptic while for  $M > 1$ , the differential equation is hyperbolic.

For the proposed study, Eq. (2) can be rewritten in a more convenient form for a supersonic unsteady flow as

$$(M^2 - 1) \phi_{xx} - \phi_{yy} - \phi_{zz} = -\frac{1}{c^2} (2 V \phi_{xt} + \phi_{tt}) \quad (3)$$

Because of its hyperbolic nature, the equation is to be satisfied only within a characteristic region, in contrast to the entire domain as in the elliptic case. This region is the downstream Mach cone originating from the source of distribution. Conversely, a receiving point in the downstream location would be affected only by disturbances generated within the upstream Mach cone of the receiving point.

For an external flow, any solution  $\phi$  to Eq. (3) would also have to satisfy the boundary conditions. For the region ahead of the downstream Mach lines from the leading edge of the surface the freestream condition should prevail. The disturbances behind these downstream Mach lines must be directed outward from their sources. The tangency condition at the surface is given by

$$w(x, y, 0, t) = \frac{D}{Dt} z(x, y, t) \quad (4)$$

where  $w$  is the perturbation velocity in the  $z$ -direction, and  $z(x, y, t)$  represents the instantaneous displacement of the mean surface normal to the  $x$ - $y$  plane.  $D/Dt$  is the substantial differential operator:

The pressure coefficient is related to  $\phi$  by

$$C_p = -\frac{2}{V^2} \frac{D\phi}{Dt} \quad (5)$$

Equation (3) as written is completely general within the framework of small perturbation theory. It admits quite an arbitrary variation in time and space for  $\phi$ . To make the problem more tractable, a more restrictive and yet practical assumption of simple harmonic motion of the airfoil is usually made. The condition is expressed as

$$z(x, y, t) = \bar{z}(x, y) e^{i\omega t} \quad (6)$$

where  $i = \sqrt{-1}$  and  $\omega$  is the frequency of the motion.  $\bar{z}(x, y)$  is called the modal deflection which can be prescribed by some polynomial representation.

If the disturbance is due entirely to simple harmonic motion, it follows that the effect as expressed by  $\phi$  would also be harmonic, i.e.,

$$\phi(x, y, z, t) = \bar{\phi}(x, y, z) e^{i\omega t} \quad (7)$$

Substituting Eq. (7) into Eq. (3), one gets

$$\beta^2 \bar{\phi}_{xx} - \bar{\phi}_{yy} - \bar{\phi}_{zz} = -\frac{1}{2} (2 i\omega V \bar{\phi}_x - \omega^2 \bar{\phi}) \quad (8)$$

where

$$\beta = \sqrt{M^2 - 1}$$

and  $\bar{\phi}(x, y, z)$  is the complex velocity potential.

Consistent with the small perturbation theory, the substantial differential operator  $\frac{D}{Dt}$  is given as:

$$\begin{aligned}
\frac{D}{Dt} &= \frac{\partial}{\partial t} + V \frac{\partial}{\partial x} \\
&= i\omega + V \frac{\partial}{\partial x} \\
&= V \left( \frac{\partial}{\partial x} + \frac{i\omega}{V} \right)
\end{aligned}$$

where second order terms have been neglected. Thus, the tangency condition (Eq. (4)) becomes

$$w(x, y, 0, t) = V \left( \frac{\partial}{\partial x} + \frac{i\omega}{V} \right) \bar{z}(x, y) \quad (9)$$

and the pressure coefficient (Eq. (5)) becomes

$$C_p = -\frac{2}{V} \left( \frac{\partial}{\partial x} + \frac{i\omega}{V} \right) \bar{\phi}(x, y, z) \quad (10)$$

Equations (8), (9) and (10) form the framework for the lifting surface theory formulated in terms of the velocity potential.

## 2.2 Acceleration Potential

From Euler's equation, Prandtl introduced the concept of acceleration potential

$$\begin{aligned}
\psi &= -\frac{p}{\rho_\infty} \\
&= \frac{\partial \phi}{\partial t} + V \frac{\partial \phi}{\partial x}
\end{aligned} \quad (11)$$

Under the small perturbation assumption,  $\psi$  also satisfies the same linear differential equation as Eq. (3). Following a similar development as for  $\phi$ , one obtains

$$\beta^2 \bar{\Psi}_{xx} - \bar{\Psi}_{yy} - \bar{\Psi}_{zz} = -\frac{1}{c^2} (2i\omega V \bar{\Psi}_x - \omega^2 \bar{\Psi}) \quad (12)$$

$$C_p = -\frac{2}{V^2} \bar{\Psi}(x, y, z) \quad (13)$$

The use of acceleration potential (also often referred to as pressure potential) proves to be especially simple in dealing with the wake condition in the lifting surface theory.

Since no pressure discontinuity can physically exist in the flow field other than across the lifting surface, the acceleration potential is identically zero everywhere except over the planform. The complicated problem of accounting for the wake can be avoided entirely by using the acceleration potential formulation. In the case of velocity potential, a discontinuity in velocity potential exists across the wake, and the wake has to be treated explicitly. The influence from the wake is especially important in the subsonic lifting theory due to the elliptic nature of the flow. For supersonic flow, with its hyperbolic characteristic, the wake aft of a supersonic trailing edge cannot exert any influence on the lifting surface, and may be neglected even if the velocity potential formulation is used. However, if the trailing edge is subsonic, the forward Mach cone extending from a receiving point on the trailing edge would include part of the wake into its region of influence. Thus, even for supersonic flow, the use of acceleration potential still has some definite advantage over the velocity potential in the treatment of the wake.

### 2.3 Integral Equation Approach

Instead of solving the linear partial differential equation directly in three-dimensional space with the boundary conditions imposed, the integral equation method approaches the problem from a different point of view. This approach assumes that elementary solutions of some type can be found, each to satisfy the differential equation as well as the boundary condition at infinity. Because of the linearity of the differential equation, the general solution can be built up from elementary solutions utilizing the principle of superposition. Some typical elementary solutions are the singular solutions such as source, sink, doublet

and vortex. The manner in which these elementary solutions are combined is dictated by the requirement that the yet untouched surface tangency condition be satisfied.

The larger the number of these elementary solutions used, the better would be the general solution. Instead of taking a discrete number of these, we can pass to the continuum limit by replacing the summation over discrete quantities by the integral over a spatial distribution of such quantities. This accounts for the appearance of the integral. In summary, this can be viewed as a building up of the solution by some known elementary solution. The problem of solving for the solution becomes a problem of how to combine the elementary solutions to achieve satisfaction of the surface boundary condition.

The integral equation puts the solution in an elegant form. An essentially three-dimensional problem is reduced by one dimension to a surface integral. However, the integral normally contains singularities and defies analytical treatment. It is interesting to point out that when one resorts to numerical integration, one has to essentially convert the continuous distribution to some discrete distribution, thus reversing the process used in setting up the integral. The whole lifting surface theory in the last two decades was evolved around evaluating such an integral representation. Such an approach is popular because while the outer boundary extends to infinity, the quantities of interest are only those evaluated on the wing surfaces such as the surface pressure distribution, etc., which can readily be evaluated from the integral approach.

The integral equation can also be derived more mathematically from the differential equation by Green's function method. However, for such a method to be applicable, the differential equation must also necessarily be linear.

Because of the use of superposition procedures, the lifting theory is mathematically limited to the linearized (small perturbation) potential flow. As such, it obviously has its limitation and may not be capable of fully describing the flow field in general. Nevertheless, due to its simplicity and computational efficiency, it can serve its purpose quite well as a design tool rather than a detailed flow

analyzer. Short of using a three-dimensional finite difference analysis, which would involve a prohibitive amount of computer time, so far there is no better nor more economical method than the lifting theory in studying the three-dimensional wing.

### SECTION III EXISTING METHODS

The object of the lifting surface theory is to seek the lift distribution corresponding to some prescribed downwash distribution. The solution is built up from elementary solutions which satisfy the linearized potential equation. For the supersonic flow, the most commonly used building blocks are the source, the potential doublet, the pressure doublet or a combination of such. Depending on the type of singular distribution used, the resulting integral equation takes on different form. The existing methods for the supersonic lifting theory can be categorized into four classes according to the integral equation used.

#### 3.1 Integrated Downwash Method

By superposition of pulsating acoustic source distribution over the lifting surface in a supersonic flow, Garrick and Rubinow (Ref. 1) derived the following equation

$$\bar{l}(x, y) = \frac{2\rho V}{\pi} \left( \frac{\partial}{\partial x} + \frac{i\omega}{V} \right) \iint_C \bar{w}(x_0, y_0) \bar{K}(x - x_0, y - y_0) dx_0 dy_0 \quad (14)$$

where  $\bar{K}(x - x_0, y - y_0)$  is the kernel function, the detail form of which is given in Garrick and Rubinow (Ref. 1), and will not be repeated here.  $C$  is the region of the surface bounded by the forward Mach lines from the point  $(x, y)$ .

As originally derived, Eq. (14) is applicable only to purely supersonic flow. The mixed supersonic case with the subsonic leading edge must be excluded. To extend the applicability to cover such a case, the Esvard concept of a diaphragm of unknown downwash is added to the given wing. The combined wing and diaphragm region has completely supersonic edges and can be treated by Eq. (14). Since  $w(x, y)$  is not known beyond the wing surface, the zero pressure difference condition instead of the downwash is imposed on the diaphragm region.

One of the earliest attempts to solve Eq. (14) for arbitrary planform is the "box" method, introduced by Pines, Dungundji and Neuringer (Ref. 2). The planform and diaphragm are divided into an aggregation of square boxes. In each box, the upwash is assumed to be constant to facilitate the integration process. The method was later improved by the use of rectangular or rhombic boxes with sides along Mach lines, the so-called characteristic boxes. Another possibility is the Mach boxes where rectangular boxes with diagonals along Mach lines are used. Zartarian and Hsu (Ref. 3) discussed the relative merits and drawbacks of each type of box. They rated the Mach box as most favorable. In the box method, since the upwash is assumed constant over the box, it can be taken out of the integral. The integration is performed just on the kernel. This can be carried out over each box in advance and the results, called the influence coefficients, can be tabulated for a unit,  $w_0$ , as a function of the position. Regardless of what box shape is used, difficulties occur for boxes which are adjacent to a subsonic leading edge. The upwash is singular in such boxes and cannot be adequately accounted for by the constant value approximation. Another shortcoming of the method is the jagged leading edge given by the box approximations, Moore and Andrew (Ref. 4) and Olsen (Ref. 5). This inexactness at the leading edge definitely affects flows downstream of the Mach cone.

Since any error at the leading edge would propagate downstream, efforts to correct the jagged leading edge were reported by Woodcock (Ref. 6). The first possibility is to take smaller boxes to reduce the jaggedness. This improves the accuracy but increases the computer time. Another approach is to use a better approximation of the upwash in the upstream part of boxes that are cut by the edge. The approximation is made to possess the inverse square root behavior at the leading edge. A third method is to weight the influence coefficient by the fraction of the box located on the wing.

In some respects, the box method can be classified as a primitive finite element method. When the shapes of the boxes are relaxed and the approximation of the upwash within each box is of a higher order than constant values, we have the classical finite element method. Appa and Smith (Ref. 7) used the quadratic

non-conforming triangular elements to calculate unsteady supersonic aerodynamic coefficients from Eq. (14). Elements on the planform need not be the same as those on the diaphragm. As a result the elements can be so arranged that no partial element would occur at the leading edge. The downwash is continuous over the planform instead of assuming discontinuous jumps as in the box method. All these contribute to a smooth pressure distribution and more accurate results. It can thus be concluded that any attempt to a higher order "box" method should be done within the theory of the finite element method.

The assessment of the integrated downwash method is summarized below.

Advantages:

- For the purely supersonic case, the method is both fast and simple. Instead of solving an integral equation, the solution is obtained successively by repeated evaluation of the surface integral.
- By discretizing the planform into boxes, the method is applicable to arbitrary planforms.

Disadvantages:

- In the box method, the constant downwash assumption was conceived for computational convenience on a desk calculator. This gives rise to jumps in downwash across adjacent boxes, which is not physically meaningful. Improved later by linear variation in the linear finite element approach, downwash is now piecewise continuous but still lacks smoothness.
- The integral relationship was originally developed for the purely supersonic case. To cover the mixed case, a diaphragm must be incorporated into the problem. The location of this diaphragm region is not unique for complex configurations, and its size could be almost as large as the planform at low supersonic Mach numbers.
- Since the downwash does not vanish in the wake region, the wake must be explicitly treated if it is contained within the forward Mach cone of a receiving point.
- For the mixed case, the velocity potentials can no longer be solved successively but require a matrix solution. This is because the downwash on the diaphragm is not known and only the condition of zero lift prevails on the diaphragm.

- Boxes have an inherent geometric problem in fitting the planform. The situation is improved by the use of finite elements.

### 3.2 Kernel Function Method

Watkins and Berman (Ref. 8) used a distribution of pressure doublets to solve the acceleration potential equation. The resulting integral equation is of the form

$$w(x, y) = \frac{1}{4\pi} \iint_C l(x_0, y_0) K(x - x_0, y - y_0) dx_0 dy_0 \quad (15)$$

where  $C$  is the planform cut off by the forward Mach cone from the point  $(x, y)$ , and  $K$  is the kernel function, the detail of which is given in Ref. (8).

Equation (15) is also applicable to the subsonic lifting theory if the supersonic kernel is replaced by its subsonic counterpart. In fact, much of the subsonic lifting calculations are solved by the kernel function method. Such a method can, with some modification, be extended to the supersonic case. The method requires that the lift,  $l$ , be expressed as a linear combination of suitably preselected functions with undetermined coefficients. The coefficients are determined by satisfying the tangency condition in some approximate fashion, e.g., collocation. The choice of the trial functions is usually based on the experience with incompressible flow and the lifting line theory. They must vary in a certain manner at the boundary of the planform to satisfy the edge conditions.

Cunningham (Ref. 9) based his pressure series upon the potential solution for triangular wings with subsonic leading edges. No separation of chordwise and spanwise variables was assumed. Curtis and Lingard (Ref. 10) chose the pressure series similar to the one in the subsonic case where separation of chordwise and spanwise variables was assumed. The series is given as a truncated, double Fourier series multiplied by suitable functions to take into account the behavior of the pressure distribution at the leading, trailing and side edges of the planform. Harris (Ref. 11) interpolated the pressure series by orthogonal

polynomials multiplied by some weighting function and chose the interpolating points at the zeros of the orthogonal polynomials. The weighting function was to assure proper behavior at edges. The interpolation was done under the assumption that chordwise and spanwise variables can be treated separately. Thus, it can be said that the choice is rather arbitrary, which is characteristic of this type of semi-analytical method.

The most costly operation is in the evaluation of the surface integral. The Gaussian-type quadrature, modified to take into account the singularity of minus one-half power at the leading edge, is usually employed. After the integration is performed, the undetermined coefficients are determined usually by the collocation method. The collocation points are usually determined on the basis of two-dimensional, steady flow theory. The resulting system of algebraic equations is to be solved for the coefficients. For  $N$  collocation points, the coefficient matrix is  $N \times N$  and full, thus the solution becomes very expensive as  $N$  gets very large.

All the above pressure series are smooth and are slow to converge to the true discontinuous pressure distribution. Recently, Cunningham (Ref. 12) devised a pressure series in which the pressure series based on Chebyshev polynomials is weighted by some discontinuous function. The weighting function is derived from supersonic conical flow theory solution. This implicit discontinuous characteristic of the pressure series gives a higher rate of convergence than its conventional counterpart.

A variant of the kernel function method is the doublet lattice method. The planform is discretized with trapezoidal panels. For subsonic flow, a line of constant doublet strength is assumed acting through the 25% chord of each panel to approximate the lift distribution. Collocation point is taken at 75% chord of each panel. The subsonic doublet lattice method, due to its generality, has been implemented in NASTRAN (Ref. 13). Harder, MacNeal and Rodden (Ref. 14) showed that a straight forward extension of the method to the supersonic flow is not feasible due to the singularity of the kernel along the forward Mach cone of the collocating point. They proposed to use Woodward's constant pressure panel (Ref. 15) for supersonic application but no result was given. Nevertheless,

in a recent paper, Brock and Griffin (Ref. 16) attempted the direct extension of the doublet lattice method to the supersonic case. While the collocation point is kept at 75% chord, it was found that better results were obtained for supersonic flow if the line of doublet is placed at 50% chord of each panel. No conclusive explanation was given.

The kernel function method is assessed below:

Advantages:

- The lift distribution is treated directly as the unknown. A  $C^0$  approximation to the lift is sufficient as well as consistent with the linearized supersonic flow theory.
- Since there is no lift off the planform, it is not necessary to treat the wake nor to incorporate a diaphragm into the analysis.
- The subsonic kernel function method is well developed. The supersonic case retains essentially the same form. Since kernels have also been formulated for transonic and nonplanar cases, the kernel function method offers a possibility of a unified approach.
- The discretization as in the doublet lattice method helps to generalize the kernel function method.

Disadvantages.

- The loading functions have to be assumed according to the planform and edge conditions. For any change in planform or in edge condition, a new set of loading functions is required. The method suffers from a lack of generality.
- The loading functions used have traditionally been smooth and continuous, which can hardly approximate the actual piecewise continuous nature of the loading in supersonic flow. The situation can be improved by incorporating some piecewise continuous weighting function from the conical flow theory.
- A matrix equation must be solved to determine the unknown coefficients.
- The location for the placement of the line of doublet appears to be arbitrary. In any case, the lift distribution has discontinuous jumps in values from panel to panel.

### 3.3 Integrated Potential Method

Based on the generalized Green's theorem, W. P. Jones (Ref. 17) derived an integral equation relating the downwash to a distribution of velocity potential doublets. Since the velocity potential doublet vanishes on the diaphragm, no diaphragm region needs to be considered. However, the wake region still has to be treated.

Allen and Sadler (Ref. 18) used a characteristic mesh and approximated the unknown potential over each rhombus by some linear or parabolic interpolation involving the undetermined potentials at the nodes of the rhombus. It is remarkable that as early as 1963, they developed what is now commonly known as the shape function in the finite element method. Allen and Sadler proceeded to solve the nodal potentials successively by collocation at the nodes, starting at the foremost point and progressing backward along the Mach lines. Woodcock (Ref. 19) used a similar procedure, incorporating minor improvements.

Two recent integrated potential methods are those by Appa and Jones (Ref. 20) and Giesing and Kalman (Ref. 21). Essentially both approaches imply a linear finite element approximation for the velocity potential doublet distribution. Appa and Jones used non-uniform characteristic mesh with the vertices as collocation points. Giesing and Kalman used trapezoidal elements and set the collocation point at 95% chord point on the boxes. Instead of solving the unknown potential in succession, both approaches generate a set of equations and the potential is solved simultaneously.

The integrated potential method is assessed below.

#### Advantages

- No diaphragm is needed.
- In the approach by Allen and Sadler, the solution is obtained successively from leading edge to trailing edge.
- The formulation is more general and is not limited to planar case alone.

Disadvantages:

- The wake region still has to be treated.
- The  $C^0$  approximation of the velocity potential gives rise to finite jumps or discontinuity in the pressure field. To obtain a meaningful piecewise continuous pressure field, a  $C^1$  approximation of the velocity potential must be employed.
- In the approaches of Appa and Jones, and Giesing and Kalman, a matrix equation must be solved.

3.4 General Theory of Unsteady Compressible Potential Aerodynamics

Chen, Suciú and Morino (Ref. 22) presented a general formulation for steady and oscillatory, subsonic and supersonic flow around complex configurations. Applying the Green function on the linearized velocity potential equation, they obtained a representation for the potential at a control point in terms of the potential and its normal derivative on the surface of the body and wake. This is equivalent to a distribution of a combination of sources and potential doublets. Instead of imposing the usual downwash boundary condition, they obtained an integral equation by requiring the potential to be continuous as the control point approaches the surface. A finite element approach with collocation is used to obtain the solution by solving a set of equations.

This method is assessed below:

Advantages:

- The formulation is unified for subsonic and supersonic flow.
- The theory is applicable to non-planar complex configurations. The thickness effect can be included.

Disadvantages:

- The wake and diaphragm region must be incorporated into the analysis.
- Zeroth order finite element approximation is used for the potential.
- The pressure is obtained by further differencing the potentials after they are determined.
- A matrix equation must be solved in the solution process.

### 3.5 Recommendations

Based on the assessments outlined in previous sections, it is concluded that any prospective method should have the following desirable features:

1. Eliminate the diaphragm and wake region.
2. Solve for the unknown lift directly.
3. Offer unified approach for subsonic and supersonic flow, and possibly transonic flow.
4. Extend to non-planar and interfering cases.
5. Adopt finite element discretization to make it applicable to arbitrary planform.
6. Avoid any matrix inversion from the solution process to save computer time and storage.

The kernel function method comes closest to satisfying all the above requirements, except the last two. In the next section, the finite element technique is applied to the kernel function method to make it more tractable by modern computers, and help fulfill the last two requirements.

## SECTION IV PRESENT METHOD

In this section, a new computational method is presented. By using a finite element approach to the kernel function method, some of the inherent shortcomings of the latter method are removed.

### 4.1 Theoretical Considerations

The present method is largely motivated by the success of the finite element method in replacing the Classical Rayleigh-Ritz method. The difficult and sometimes impossible task of choosing the appropriate trial functions is conveniently replaced by a systematic and general piecewise polynomial approximation over the discretized domain.

The method is further guided by the theory of characteristics which says that flow properties, such as the velocities and pressure, while continuous may not have continuous first derivatives across characteristic lines. Mathematically, this means flow properties are  $C^0$  continuous in supersonic flow. Since the theory of characteristics is also based on the same linearized differential equation, this property has to be observed even in the integral approach. Thus, the lift distribution, instead of smooth as in the subsonic case, is now  $C^0$  continuous for supersonic flow. Fortunately, most of the shape functions in finite element method belong to the  $C^0$  class. In fact, it would be much more difficult to devise a  $C^1$  continuous shape function.

Based on these considerations, the finite element shape functions can advantageously be applied to the kernel function method.

#### 4.2 Statement of the Problem

The integral equation relating the complex upwash  $Vw(x, y)e^{i\omega t}$  to the load distribution  $\rho V^2 l e^{i\omega t}$  for the supersonic lifting surface theory is given in the AGARD notation (Ref. 6) as

$$w(x, y) = \frac{1}{4\pi} \iint_C l(x_0, y_0) K(x - x_0, y - y_0) dx_0 dy_0 \quad (16)$$

where  $C$  is the area of the planform cut off by the forward Mach cone from the point  $(x, y)$ .

The oscillatory supersonic kernel function  $K$  for a planar surface is given in the form

$$\begin{aligned} K(x, y) &= \frac{2e^{-i\omega x/V}}{y^2} \left[ \frac{x}{R} \cos\left(\frac{\omega MR}{\beta^2 V}\right) \exp\left\{\frac{-i\omega x}{\beta^2 V}\right\} \right. \\ &\quad \left. + \frac{i\omega}{2V} \int_{(x-MR)/\beta^2}^{(x+MR)/\beta^2} \frac{\exp\left\{\frac{i\omega u}{V}\right\} u du}{(u^2 + y^2)^{1/2}} \right] \quad (x > \beta|y|, y \neq 0) \\ &= \frac{2e^{-i\omega x/V}}{y^2} \quad (x > \beta|y|, y = 0) \\ &= 0 \quad (x \leq \beta|y|) \end{aligned}$$

where

$$R = \sqrt{x^2 - \beta^2 y^2} \quad (17)$$

Let the vertical displacement of the lifting surface be expressed as

$$Z(x, y, t) = s \sum_i f_i(x, y) q_i(t) \quad (18)$$

where  $s$  is the wing semi-span, the  $f_i(x, y)$  are the (dimensionless) modal functions and the  $q_i(t)$  are the (dimensionless) generalized coordinates.

The nondimensionalized upwash on the lifting surface is

$$\begin{aligned} w(x, y, 0, t) &= \frac{dz}{dt} \\ &= \left( ik + \frac{\partial}{\partial x} \right) \frac{Z(x, y, t)}{s} \\ &= \left( ik + \frac{\partial}{\partial x} \right) \sum_i f_i(x, y) q_i(t) \end{aligned} \quad (19)$$

Thus for the  $i^{\text{th}}$  mode, the corresponding upwash is

$$w_i(x, y, 0, t) = \left( ik + \frac{\partial}{\partial x} \right) f_i(x, y) q_i(t) \quad (20)$$

Substituting this in the integral equation, one obtains for the  $i^{\text{th}}$  mode shape

$$\left( \frac{\partial}{\partial x} + ik \right) f_i(x, y) q_i(t) = \frac{1}{4\pi} \iint_C t_i(x_0, y_0) K(x - x_0, y - y_0) dx_0 dy_0 \quad (21)$$

Equation (21) can be rearranged as

$$\left(\frac{\partial}{\partial x} + ik\right) f_i(x, y) = \frac{1}{4\pi} \iint_C \frac{\ell_i(x_0, y_0)}{q_i(t)} K(x - x_0, y - y_0) dx_0 dy_0 \quad (22)$$

By defining  $\lambda_i(x_0, y_0) = \ell_i(x_0, y_0)/q_i(t)$ , which can be interpreted as the lift distribution due to a unit displacement in the  $i^{\text{th}}$  generalized coordinate, the working form of the integral equation becomes

$$\left(\frac{\partial}{\partial x} + ik\right) f_i(x, y) = \frac{1}{4\pi} \iint \lambda_i(x_0, y_0) K(x - x_0, y - y_0) dx_0 dy_0 \quad (23)$$

For aeroelastic analysis, the aerodynamic forces are conventionally input in the form of some integrated force coefficients rather than actual lift distribution. The AGARD definition of the generalized force coefficients is

$$Q_{ij} = - \int_{-1}^1 \int_{x_{1e}}^{x_{te}} f_i(x, y) \lambda_j(x, y) dx dy \quad (24)$$

where  $f_i(x, y)$  are the  $i^{\text{th}}$  modal functions and  $\rho V^2 \lambda_j(x, y) q_j(t)$  is the contribution to the vertical force per unit area resulting from harmonic oscillation in the  $j^{\text{th}}$  degree of freedom (i.e. with  $q_j(t) = q_{j0} e^{i\omega t}$ ).

The complex  $Q_{ij}$  is conventionally written as

$$Q_{ij} = Q'_{ij} + ik Q''_{ij} \quad (25)$$

where

$$Q'_{ij} = \text{Re}(Q_{ij})$$

and

$$Q_{ij}'' = \Im m(Q_{ij}')/k$$

with

$$k = \omega s/V, \text{ the reduced frequency}$$

Given a set of modal functions,  $f_i$ , the geometry of the planform, the free-stream Mach number and the reduced frequency, the problem is to solve Eq. (23) to obtain  $\lambda_i$ . This is subsequently input into Eq. (24) to compute the generalized force coefficients  $Q_{ij}'$  and  $Q_{ij}''$ .

#### 4.3 Finite Element Formulation

The first step in the finite element approach is to discretize the planform into finite elements. With arbitrary aligned elements, since the region of integration is limited to the forward Mach cone, elements on the Mach cone boundary would be partially cut by the Mach cone (Fig. 1). The partially cut elements would have to be determined prior to the integration process for each collocation point. Clearly this would involve a considerable amount of bookkeeping, not to mention the labor in determining the intersections. On the other hand if all the elements are bounded by characteristic lines, it becomes a clearcut decision as to whether the element is to be included in the integration. For this method, a characteristic mesh would be used exclusively.

After the planform is discretized into elements, the surface integral can be replaced by a summation of surface integrals over each element contained within the forward Mach cone. Equation (23) becomes

$$\left(\frac{\partial}{\partial x} + ik\right) f_i(x, y) = \frac{1}{4\pi} \sum^{(e)} \iint_{A^{(e)}} \lambda_i^{(e)}(x_0, y_0) K(x - x_0, y - y_0) dA \quad (26)$$

where  $\lambda_i^{(e)}$  is the local lift distribution over the element and  $\sum^{(e)}$  denotes summation over elements within the forward Mach cone. The local lift distribution can be replaced by the finite element approximation as

$$\lambda_i^{(e)}(x_o, y_o) = \bar{N}^t(x_o, y_o) \cdot \bar{\lambda}_i^{(e)} \quad (27)$$

where  $\bar{N}^t$  is the row vector of shape function and  $\bar{\lambda}_i^{(e)}$  is the column vector of nodal lift values.

Substituting Eq. (27) into Eq. (26), one obtains the finite element form of the integral equation

$$\left(\frac{\partial}{\partial x} + ik\right) f_i(x, y) = \frac{1}{4\pi} \sum^{(e)} \iint_{A^{(e)}} \bar{N}^t(x_o, y_o) K(x-x_o, y-y_o) dA \cdot \bar{\lambda}_i^{(e)} \quad (28)$$

One immediate consequence is that the integrand no longer contains the unknown lift distribution. It depends only on the relative position between the influencing element and the collocation point, and can be evaluated readily with proper attention to the singularities in the kernel function.

For convenience, define the integrated values of the product of shape functions and kernel function as the weighted kernel coefficients, i.e.,

$$\bar{C}^t(e) = \iint_{A^{(e)}} \bar{N}^t(x_o, y_o) K(x-x_o, y-y_o) dA \quad (29)$$

The integral equation finally becomes

$$\left(\frac{\partial}{\partial x} + ik\right) f_i(x, y) = \frac{1}{4\pi} \sum^{(e)} \bar{C}^t(e) \cdot \bar{\lambda}_i^{(e)} \quad (30)$$

With the finite element approximation, the generalized force coefficients are

$$Q_{ij} = -\sum_{n=1}^N \iint_{A^{(e)}} f_i(x, y) \bar{N}^{(t)}(x, y) dx dy \cdot \bar{\lambda}_j^{(e)} \quad (31)$$

where  $\sum_{n=1}^N$  denotes summation over all the elements on the planform.

Equations (29), (30), and (31) represent the finite element formulation of the lifting surface theory.

#### 4.4 Choice of Elements

Originally it was thought that by using higher order triangular and quadrilateral elements, fewer nodes are required to generate results of the same accuracy. While this is true in general, it is not suitable for the type of solution process used in this method.

Since the nodes are to be used as collocation points, the additional nodes on the side would have their forward Mach cones cutting through the elements (Fig. 2). Also, since the nodal variables of the same element are dependent on each other, all the unknown nodal variables would have to be solved simultaneously for each element. For example, if quadratic elements are used, at each stage there would be three unknown nodal variables to be determined simultaneously. Whereas, if linear elements are used, there would be just one unknown nodal variable to be determined at each stage. The net saving by using higher order elements in eliminating the interior nodes can hardly justify the additional work. Also, the parametric property of the higher order elements, which can be used to fit curve characteristics, can hardly be utilized in this study since the Mach number remains constant over a supersonic planar surface. With due consideration to all these problems, it was concluded that the linear finite elements can best serve our solution technique.

#### 4.5 Choice of Mesh

The nonuniform element mesh was initially considered since it would provide an added flexibility in fitting the actual planform (Fig. 3). While this is technically feasible, it was not adopted due to economic reasons. For each collocation point, every element contained in the forward Mach cone must be integrated. The surface integral is usually done numerically through the use of Gaussian quadratures. Since the integrand contains the kernel function with its singularities, a high order Gaussian quadrature has to be employed to get a meaningful representation. As one marches downstream to the trailing edge, more and more elements are included in the Mach cone. The costly numerical integration has to be performed over and over even for the same element since the relative position of the receiving point is changing each time. For a coarse mesh, this does not present much of a problem. If the mesh has to be refined for better accuracy, which is almost mandatory for unsteady flow at high frequency, the wastefulness of such nonuniform mesh becomes clear. In an effort to reduce the computer time, it was realized that since the kernel function is a function only of the relative location between the receiving point and the sending point, much of the duplicated effort in the numerical integration can be avoided by using a uniform mesh. Essentially a stencil of uniform elements large enough to cover the most extreme cases is set up and the integrated values are stored in a table. For each receiving point, the integration over regular elements can be replaced simply by a table look-up, with the necessary numerical integration performed only on the irregular elements. With such an approach, much saving in computer time can be realized.

For the rectangular wing, since the planform edges are composed of either horizontal or vertical lines, the mesh can be arranged such that the edges cut the characteristic boxes regularly across the vertices. As a result, only a combination of characteristic boxes and regular triangular elements is necessary to fit the planform exactly (Fig. 4). However, for the non-rectangular planform, since the edges are inclined at arbitrary angles, they

cut the boxes across the sides at several possible locations (Fig. 5). This gives rise to the possibility of having a partially cut element with five vertices.

Some effort was spent in developing subroutines to handle these irregular polygons. If the inverse square singularity does not pass through these elements, they can easily be treated. For example, the five-sided element can be treated as a combination of triangle and quadrilateral. However, for singular elements, some additional problems arose. Since the width of the singular strip is limited by the proximity of the nodes, some situation might arise where the strip has to be taken extremely small. Tests on the subroutines indicated that for such extreme cases, the nodal values of the integrated kernel can become extremely large in magnitude and unreliable. It should be pointed out here that in Appa's finite element approach on the integrated downwash method (Ref. 7), it was possible to fit the planform exactly mainly because the only singularity is of the inverse square root type, which is integrable, and not of the inverse square type, which necessitates the use of Cauchy principal value.

To keep the program simple, it was then decided to use just the type of elements which have been proved successful with the rectangular wing. For the non-rectangular wing, this gives rise to the jagged leading edge, a common undesirable feature of all box methods. However, with the finite element technique, by introducing triangular fill-in elements, the jaggedness at the planform edge is substantially reduced. The method, in effect, combines the best features of the Mach box method and the characteristic box method. For example, it can approximate a rectangular wing as exactly as the Mach box method, while it can also handle sonic edges as well as the characteristic box method.

#### 4.6 Finite Element Integration Scheme

The supersonic kernel function has a singularity of the type  $\lim_{\epsilon \rightarrow 0} \frac{1}{\epsilon^2}$  along the line extending from the collocation point in the upstream direction.

This inverse square singularity is not integrable in the usual sense, and the improper integral must be evaluated using the concept of Cauchy's principal value.

The supersonic kernel function has an additional singularity of the type  $\lim_{\epsilon \rightarrow 0} \frac{1}{\sqrt{\epsilon}}$  along the forward Mach cone boundary. Fortunately, this type of singularity is integrable and can easily be treated by the Gaussian type quadrature.

In the conventional kernel function method, the area of integration is divided into sub-regions such that the spanwise singularity is confined within a narrow strip (Fig. 6). For regions other than this strip the integral is not singular and the integration can be carried out individually. Care must be taken to apply the proper integration limits which are dependent on the planform geometry and the location of the control point. Treatment of the singular strip falls into two categories. The first method is to carry out the chordwise integration in conjunction with a Lagrange interpolation in the spanwise direction. The resulting polynomial is then integrated using the Cauchy principal value to extract the finite part of the improper integral. The second method is to subtract and add a term which mimics the integrand at the singularity. The original integrand with the singularity subtracted is now well behaved and can be evaluated numerically. The correction term which contains a simpler integrand can be evaluated analytically using the Cauchy principal value.

In the finite element approach, since the local approximation is used, it would be more efficient to perform the integration on an element-to-element basis. Since a uniform characteristic mesh of linear elements is used, the nodes are arranged in a regular pattern. The singular strip is taken to be a fraction of the element half width. If the singular strip passes through an element, it does so regularly through the middle nodes or through either extreme nodes. (Fig. 7). For such singular elements, the integration is performed by first decomposing the element into sub-regions and then applying the appropriate integration scheme. For non-singular elements, a direct Gaussian integration is used

#### 4.7 Integration Across the Singular Strip

As mentioned in the last section, two methods are available for the integration across the singular strip. Due to its simplicity in implementation, the first method is adopted.

The general form of the integral across the singular strip is

$$\int_{\eta_a=y-\epsilon}^{\eta_b=y+\epsilon} \int_{\xi_a(\eta)}^{\xi_b(\eta)} \bar{N}^t(\xi, \eta) K(x, y; \xi, \eta, \omega, M) d\xi d\eta \quad (32)$$

K is the kernel function, which can be written as

$$K = \frac{1}{(y-\eta)^2} \bar{K} \quad (33)$$

where the inverse square singularity has been factored out and  $\bar{K}$  contains only integrable singularities. Equation (32) can be written as

$$\int_{y-\epsilon}^{y+\epsilon} \frac{1}{(y-\eta)^2} \int_{\xi_a(\eta)}^{\xi_b(\eta)} \bar{N}^t(\xi, \eta) \bar{K}(x, y; \xi, \eta, \omega, M) d\xi d\eta \quad (34)$$

The integral can be evaluated first by integrating in the chordwise direction  $\xi$ , and then in the spanwise direction  $\eta$ .

The chordwise integration can be replaced by some Gaussian type quadrature in the following manner

$$\begin{aligned} F(\eta) &= \int_{\xi_a(\eta)}^{\xi_b(\eta)} f(\xi, \eta) d\xi = \frac{\xi_b(\eta) - \xi_a(\eta)}{2} \int_{-1}^1 f[\xi(\zeta), \eta] d\zeta \quad (35) \\ &= \frac{\xi_b(\eta) - \xi_a(\eta)}{2} \sum_i^n w_i f_i \end{aligned}$$

with

$$\xi_i = \frac{\xi_b(\eta) - \xi_a(\eta)}{2} \zeta_i + \frac{\xi_b(\eta) + \xi_a(\eta)}{2}$$

$$f_i = f(\xi_i, \eta)$$

and  $W_i$  and  $\zeta_i$  are the weights and abscissas of the quadrature over the interval  $[-1, 1]$

The spanwise integration has the following form

$$\int_{y-\epsilon}^{y+\epsilon} \frac{F(\eta)}{(y-\eta)^2} d\eta$$

Since the inverse square singularity is an essential singularity, the integral has to be treated using Cauchy's principal part. Watkins (Ref. 23) devised a quadrature based on an equally spaced Lagrangian interpolation in conjunction with the Cauchy principal part. For a sixth degree Lagrange interpolation, the quadrature is

$$\int_{y-\epsilon}^{y+\epsilon} \frac{F(\eta)}{(y-\eta)^2} d\eta$$

$$= \frac{1}{100\epsilon} \left[ 13(F_1 + F_7) + 72(F_2 + F_6) + 495(F_3 + F_5) + (-1360) F_4 \right] \quad (36)$$

Cunningham (Ref. 9) presented a tenth degree version of the following form

$$\int_{y-\epsilon}^{y+\epsilon} \frac{F(\eta)}{(y-\eta)^2} d\eta$$

$$= \frac{1}{571,536\epsilon} \left[ 33,911(F_1 + F_{11}) + 266,500(F_2 + F_{10}) \right. \quad (37)$$

$$+ 147,375(F_3 + F_9) + 822,000(F_4 + F_8)$$

$$+ 4,562,250(F_5 + F_7)$$

$$\left. + (-12,807,144) F_6 \right]$$

The abscissas are numbered starting from  $(y-\epsilon)$  to  $(y+\epsilon)$ .  $F_1, F_2, \dots, F_n$  represent the function  $F(\eta)$  evaluated at the corresponding abscissas.

Tests showed that the sixth degree quadrature performs nearly as well as the tenth degree version. For efficiency, the sixth degree quadrature, Eq. (36), is used in present study.

#### 4.8 Starting Solution

For a hyperbolic differential equation, the initial condition is required to start the solution process, as in the method of characteristics. For the integral approach, a starting solution is seldom used. In order to take advantage of the hyperbolic nature of the flow and also to avoid any matrix inversion, a successive solution process with a starting solution is proposed.

Since the dependent variable of the kernel function method is the lift, the starting solution requires that the lift at the leading edges be specified. Adjacent to the supersonic leading edge the flow is locally two-dimensional for an

oscillating airfoil in supersonic flow, Miles (Ref. 24) gave the pressure amplitude as

$$\bar{l}(x) = a_0 g(x) \bar{v}(0+) + a_0 \int_{0+}^x g(x-\xi) [\bar{v}_\xi(\xi) + ik\bar{v}(\xi)] d\xi \quad (38)$$

where  $a_0 = 4/\beta$  is the two-dimensional (Ackeret) lift curve slope,  $\bar{v}$  is the dimensionless downwash (positive down), and

$$g(x) = \exp(-ikM^2 x/\beta^2) J_0(kMx/\beta^2) \quad (39)$$

where  $J_0$  is the Bessel function.

In AGARD convention, lift is normalized by  $\rho V^2$  instead of the usual  $\rho V^2/2$ . To account for the difference,  $a_0 = 2/\beta$  is used. Setting  $x = 0$ , the lift at a supersonic leading edge is obtained as

$$\bar{l}(0) = \frac{2}{\beta} \bar{v} \quad (40)$$

Replacing the downwash by our upwash,  $\bar{w}$ , Eq. (40) becomes

$$\bar{l} = -\frac{2}{\beta} \bar{w} \quad (41)$$

For a supersonic swept-back wing of infinite span, the lift is modified by a sweepback factor (Ref. 25)

$$\bar{l} = -\frac{2}{\beta} \bar{w} \cdot \frac{1}{\sqrt{1-n^2}} \quad (42)$$

with  $n = \frac{\tan \Lambda}{\beta}$

where  $\Lambda$  is the sweepback angle.

For a subsonic leading edge, the lift goes to infinity as  $\lim_{\epsilon \rightarrow 0} \frac{1}{\sqrt{\epsilon}}$ . Some arbitrary large number can be specified. In this case, it is very important to use the appropriate Gaussian type quadrature with the same singular behavior when performing the integration over the leading edge element.

#### 4.9 Edge Conditions and Gaussian Quadrature

In arriving at the integral equation, the boundary condition at infinity is satisfied by the judicious choice of the elementary solution such as the source or doublet. The nature of the equation, be it elliptic or hyperbolic, is taken into account by observing the proper region of integration. The tangency condition at the surface is explicitly expressed in terms of the integral equation. However, no provision was made for the edge condition. This latter condition must be incorporated as a constraint to the integral equation.

Edges are designated as subsonic or supersonic edges according to whether the normal component of the freestream velocity to the edge is subsonic or supersonic. The edge conditions for  $\Delta p$  are

- ①  $\lim_{\epsilon \rightarrow 0} \sqrt{\epsilon}$  at side edge, subsonic or sonic trailing edge
- ②  $\lim_{\epsilon \rightarrow 0} 1/\sqrt{\epsilon}$  at subsonic leading edge
- ③  $\Delta p$  finite at supersonic leading edge or supersonic trailing edge.

These conditions can be incorporated into the solution in the form of weighting functions to the edge elements.

The  $\lim_{\epsilon \rightarrow \Delta 0} 1/\sqrt{\epsilon}$  type of singularity can be handled readily by using the Gauss-Chebyshev quadrature as follows

$$\int_{-1}^1 \frac{f(x)}{\sqrt{1-x^2}} dx \cong \sum_{i=1}^n w_i f(x_i) \quad (43)$$

where

$$x_i = \cos \frac{(2i-1)\pi}{2n}$$

$$w_i = \frac{\pi}{n}$$

When applied to a function  $F(x)$  which contains implicit singularity of type

$$\frac{1}{\sqrt{1-x^2}},$$

$$\int_{-1}^1 F(x) dx = \int_{-1}^1 \frac{\sqrt{1-x^2} F(x)}{\sqrt{1-x^2}} dx \quad (44)$$

$$\cong \sum_{i=1}^n w_i \sqrt{1-x_i^2} F(x_i)$$

$$= \sum_{i=1}^n W_i F(x_i)$$

where

$$x_i = \cos \frac{(2i-1)\pi}{2n}$$

$$W_i = w_i \sqrt{1-x_i^2} = \frac{\pi}{n} \sin \frac{(2i-1)\pi}{2n}$$

One of the nicest features of the Gauss-Chebyshev quadrature is that the weights and abscissas can be generated systematically to any degree, instead of requiring a table input as with the rest of the Gaussian quadrature. In addition, it has been determined in this study that the modified Gauss-Chebyshev quadrature can also adequately approximate integrals of the type

$$\int_{-1}^1 f(x) \sqrt{1-x} dx$$

and

$$\int_{-1}^1 f(x) dx$$

For  $f(x) = 1, x$  or  $x^2$ , less than 1% relative error can be achieved with  $n \geq 12$ .

For ease of implementation, it was decided to use this "all purpose" quadrature, Eq. (44), throughout despite the fact that relatively large numbers of quadrature points are necessary.

In the solution process, the nodal lift values are initially set to zero. Nodes on the side edges are excluded from further treatment and retain their zero lift values throughout the analysis. At the leading edge, the sweepback factor,  $1/\sqrt{1-n^2}$  is first determined. For  $0 \leq n < 1$ , the leading edge is supersonic and the lift at the leading edge is given by Eq. (42), where the unswept lift is amplified by the sweepback factor. For  $n \geq 1$ , the leading edge is subsonic and

the sweepback factor becomes imaginary. The lift becomes singular at the subsonic leading edge as  $\lim_{\epsilon \rightarrow 0} C/\sqrt{\epsilon}$ , where  $C$  is an arbitrary constant of  $O(1)$ . Comparing this form with the expression of Eq. (42), one can let the sweepback factor be replaced by the factor  $\lim_{\epsilon \rightarrow 0} 1/\sqrt{\epsilon}$  for  $n \geq 1$ . It follows that  $C$  is given by the supersonic unswept value as expressed by Eq. (41). Thus, for a subsonic leading edge, the starting value is given by Eq. (41) while the factor  $1/\sqrt{\epsilon}$  is absorbed into the quadrature as a weighting function.

For a supersonic trailing edge, the computation is performed up to and including the trailing edge nodes. For subsonic or sonic trailing edge, the trailing edge nodes are excluded from the analysis and thus retain the zero lift value. This means that the lift distribution drops from a finite value to zero within the trailing edge element.

#### 4.10 Kernel Function Evaluation

The kernel function expression in Eq. (17) involves an integral which cannot be evaluated analytically. With some numerical approximation on this integral, closed form evaluation of the kernel function is possible. H. J. Cunningham presented a closed form evaluation of Eq. (17) in the appendix of Ref. (26).

Harder and Rodden (Ref. 27) obtained a more general form of the kernel function, which is reducible to Eq. (17) for the planar case. A closed form evaluation of the version by Harder and Rodden was given by A. M. Cunningham in the appendix of Ref. (12).

In the course of this study, it was found that some discrepancies exist in the values of the kernel function obtained by either procedure. Some representative values are presented in Table 1, which shows that A. M. Cunningham's version is less sensitive to changes in reduced frequency. Both versions were subsequently applied to a rectangular wing at  $M = 1.2$ . Results based on A. M. Cunningham's version gave better agreement to available data (Ref. 6),

especially for nonzero reduced frequencies. With the added advantage of extensibility to nonplanar case, A.M. Cunningham's version is adopted in this study.

#### 4.11 Solution Procedure

The solution procedure of this method is summarized as follows:

1. Based on the Mach number of the flow, set up and input the element information for the planform.
2. Input a reduced frequency and the shape modes  $f_i$  of the deflection to compute the nodal upwash for each mode.
3. Clear nodal lift values and impose starting solution at leading edge and set other side conditions.
4. Select the collocation node (NODE) starting with the foremost node with unknown lift. Set  $SUM_i = 0$ .
5. Select the influencing element.
6. Compute the weighted kernel coefficients.
7.  $SUM_i = SUM_i + \bar{C}^{t(e)} \cdot \bar{\lambda}_i^{(e)}$
8. Repeat steps 5 through 7 until all influencing elements have been accounted for.
9. Compute the unknown lift for each mode,  $i$ , according to

$$\lambda_i(\text{NODE}) = (4\pi w_i - SUM_i) / C(\text{NODE})$$

10. Repeat steps 4 through 9 until all nodes with unknown lift are accounted for.
11. Compute the generalized force coefficients.
12. Output.
13. End.

## SECTION V

### RESULTS AND DISCUSSION

A computer program (Ref. 28) based on the present method was developed and applied to the AGARD planforms which include the rectangular  $A = 2.0$ , the arrowhead  $A = 4.0$ , and the tapered swept back  $A = 1.45$ . The choice of Mach number and planform is such that all possible combination leading/trailing edge conditions are covered (see Table 2). The program was run on a UNIVAC 1108 and the statistics given in Tables 3 through 5 are based on this machine. The 15 point modified Gauss-Chebyshev quadrature was used throughout except for the Tapered Sweptback  $A = 1.45$ ,  $M = 1.04$  case, where only 12 points were used. In general, a factor of 2.5 to 3.0 reduction in time can be expected with a CDC 6600, with a slight increase in accuracy due to the larger word size in reducing the truncation error in accumulation.

Results are given in the form of generalized force coefficients. The most extensive source of generalized force coefficients is the AGARD report by Woodcock (Ref. 6). With the exception of a few cases, all the supersonic data in the report were generated from the characteristic box method (Refs. 29 and 30). Another source of data, based on the Mach box method, was provided in the report by Olsen (Ref. 5). No results based on the kernel function method are available for comparison. It appears that this work is the only one in tabulating the generalized force coefficients by the supersonic kernel function method. Thus, the two reports mentioned earlier will serve as the standard of comparison for this study.

The generalized force coefficients  $Q'_{ij}$  and  $Q''_{ij}$  are tabulated individually for each case preceded by a figure depicting the actual mesh used for each Mach number. One case is defined as one planform, at one Mach number and reduced frequency. Instead of separating the modes into symmetric sets and antisymmetric sets as in Ref. 6, only one combined set is used. It is pointed

out that in Ref. 5 the program used could not handle antisymmetric modes  $y$  and  $x$ . Consequently, the antisymmetric modes were replaced by  $|y|$  and  $x|y|$  in Ref. 5. One should take this into consideration when comparing the results. Also, the flap rotation mode in Ref. 6 is not treated in this study.

Each table is arranged such that  $Q'_{ij}$  is tabulated before  $Q''_{ij}$ . The planform, Mach number, reduced frequency and mode shapes are also specified. In addition, the mesh fineness is also specified through the length of the side of the characteristic element, DELTA.

Because of the large amount of data involved, it is not possible to discuss each case individually. In general, the present results agree reasonably well in trends with reported values. In some cases, the values fall between the reported values, while in other cases, the values are slightly off. Considering that discrepancies exist even between the two versions of the characteristic box method, the present results are very encouraging.

Some of the discrepancies can be explained readily from a mathematical point of view. The generalized force coefficients can also be interpreted as the moments of the lift distribution. In the box method, the lift distribution is approximated by some step function like distribution, since the lift is constant within each box but assumes different values from one to the other. For this type of distribution, the approximation is accurate at most to the zeroth moment. Higher moments will become less and less accurate. In comparison, the linear approximation in the present method is accurate up to the first moment.

In conclusion, since all the reported values are based on some type of box method, they tend to reinforce each other. Without further unbiased comparison from some other method, it is almost impossible to conclude which method gives the better result.

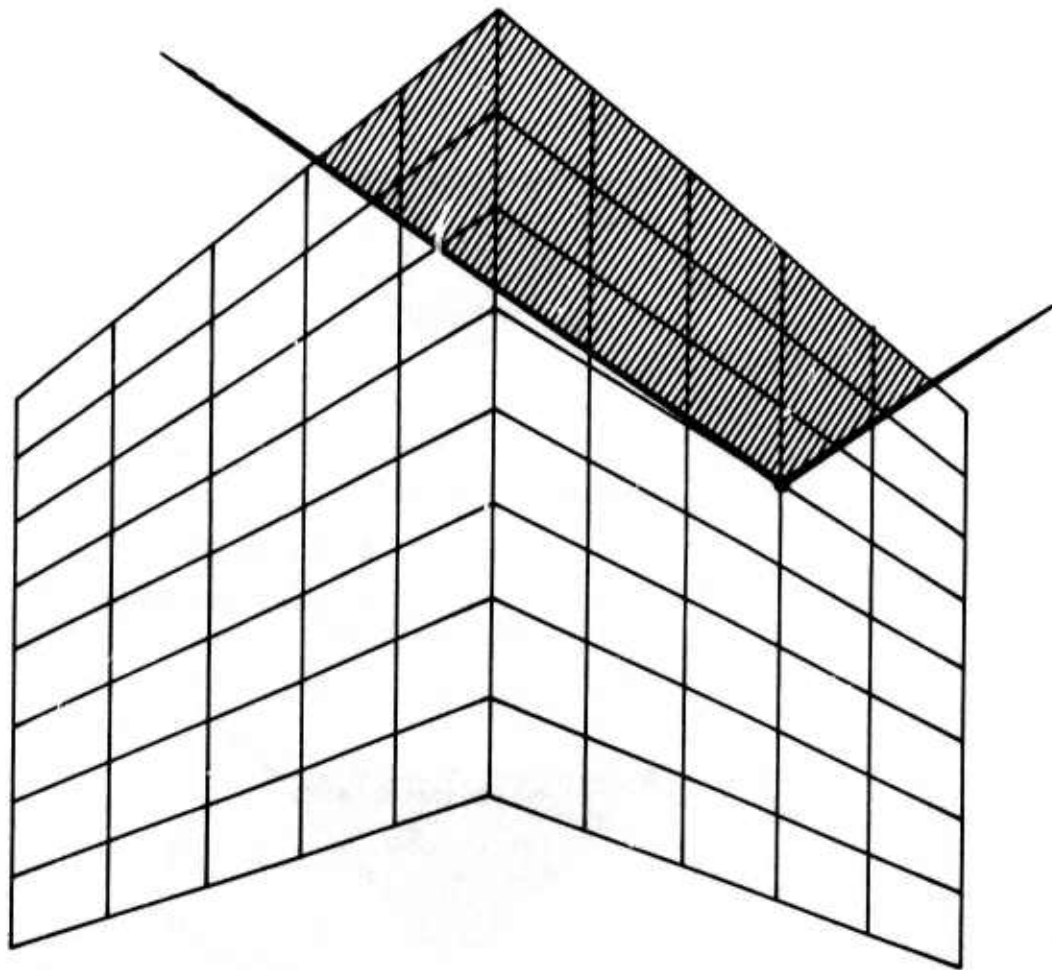
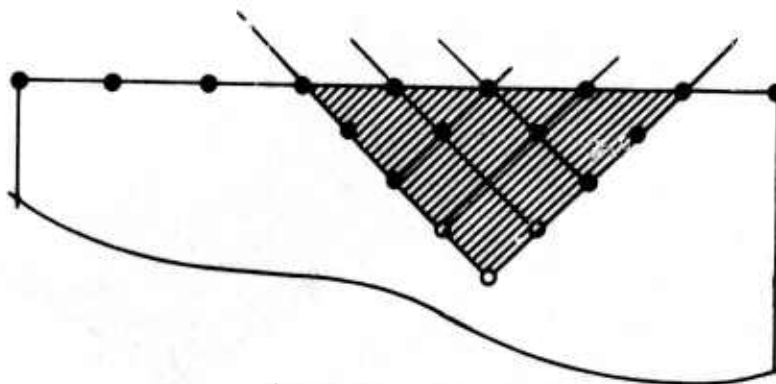
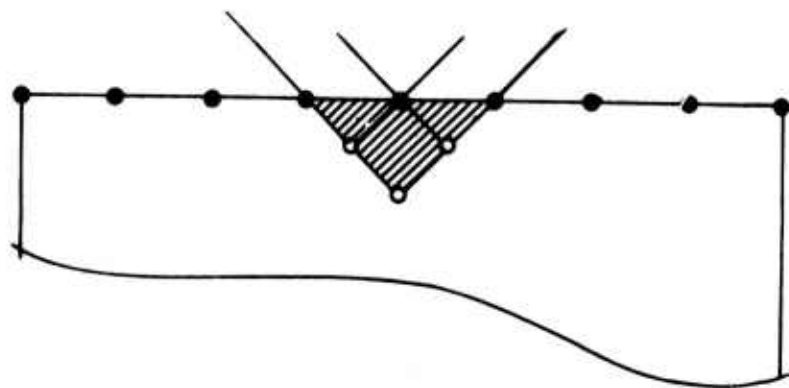
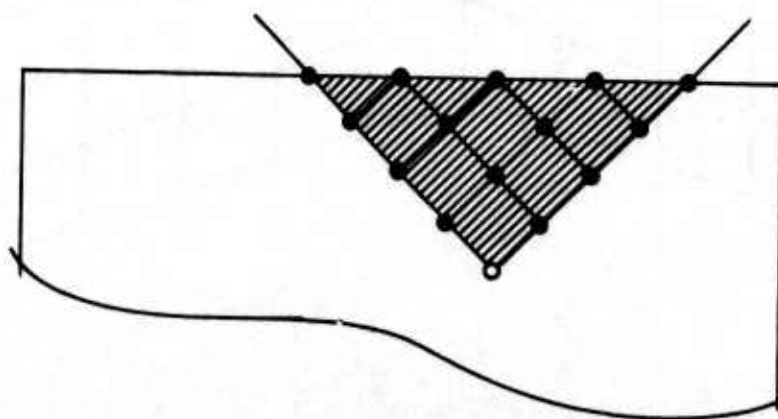


Fig. 1 - Arbitrarily Aligned Mesh



Quadratic Elements

- Known Nodal Lift
- Unknown Nodal Lift



Linear Element

Fig.2 - Quadratic Elements vs Linear Elements

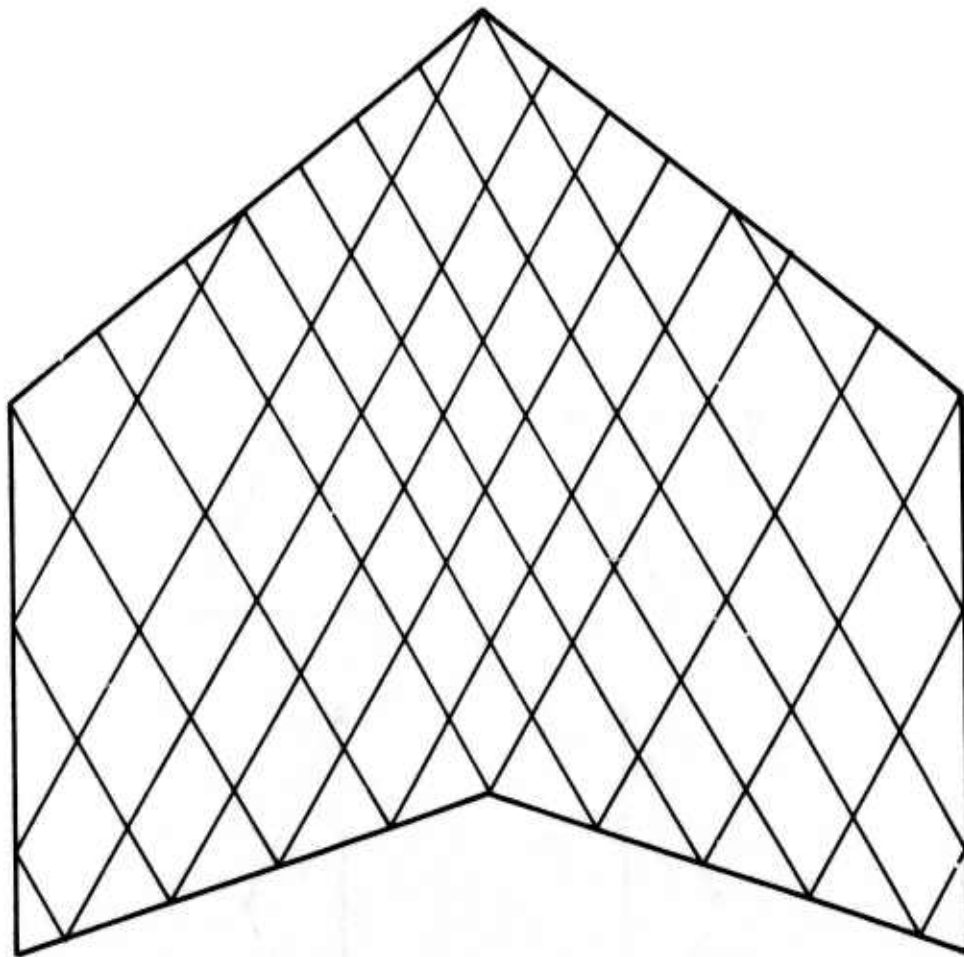
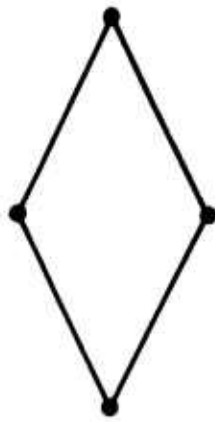
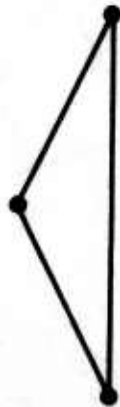


Fig. 3 - Nonuniform Mesh



Regular Characteristic Element



Triangular Fill-In Elements

Fig. 4 - Typical Elements Used to Fit the Planform

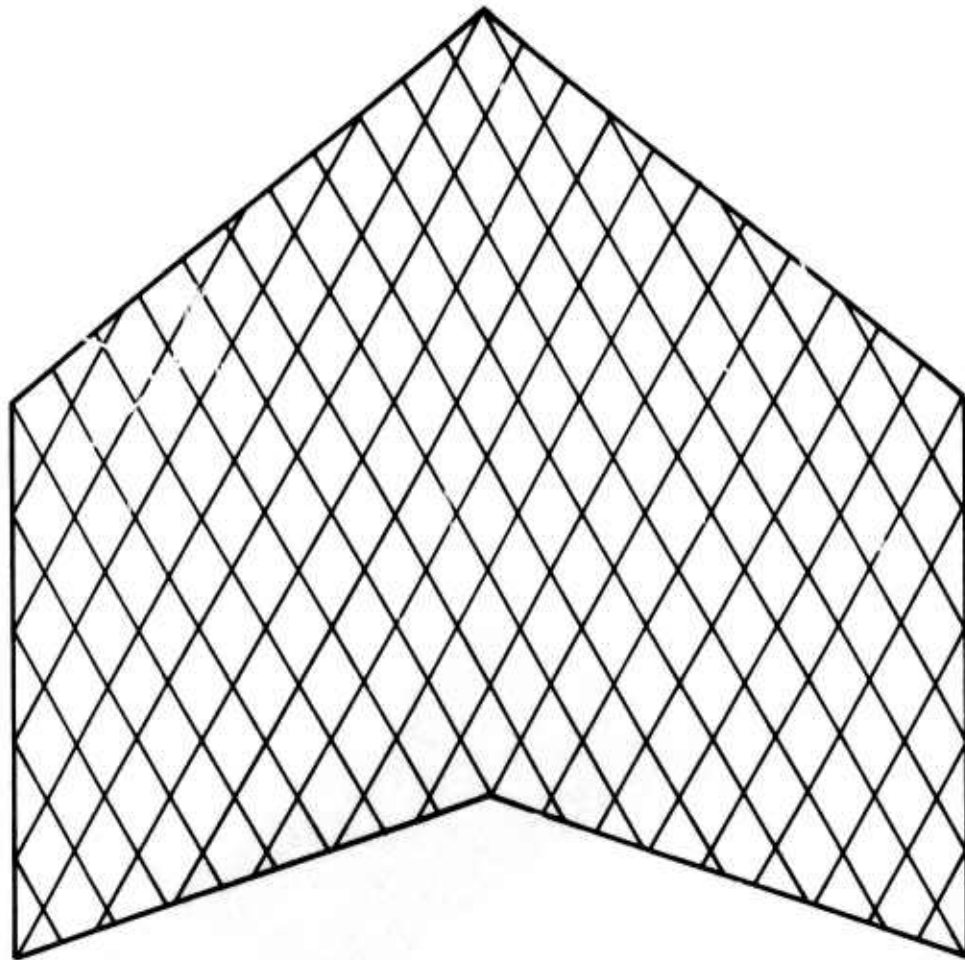


**Fig. 5 - Regular Mesh with Irregular Elements at Planform Edges  
(Note the occurrence of elements with five vertices).**

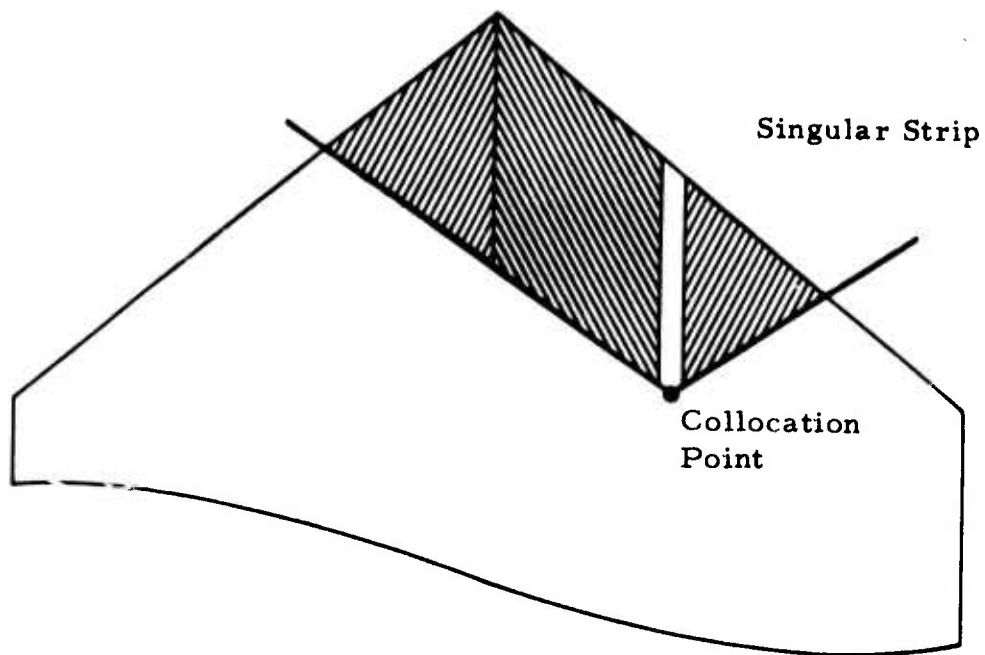


Fig. 6 - Regions of Integration for Conventional Kernel Function Method

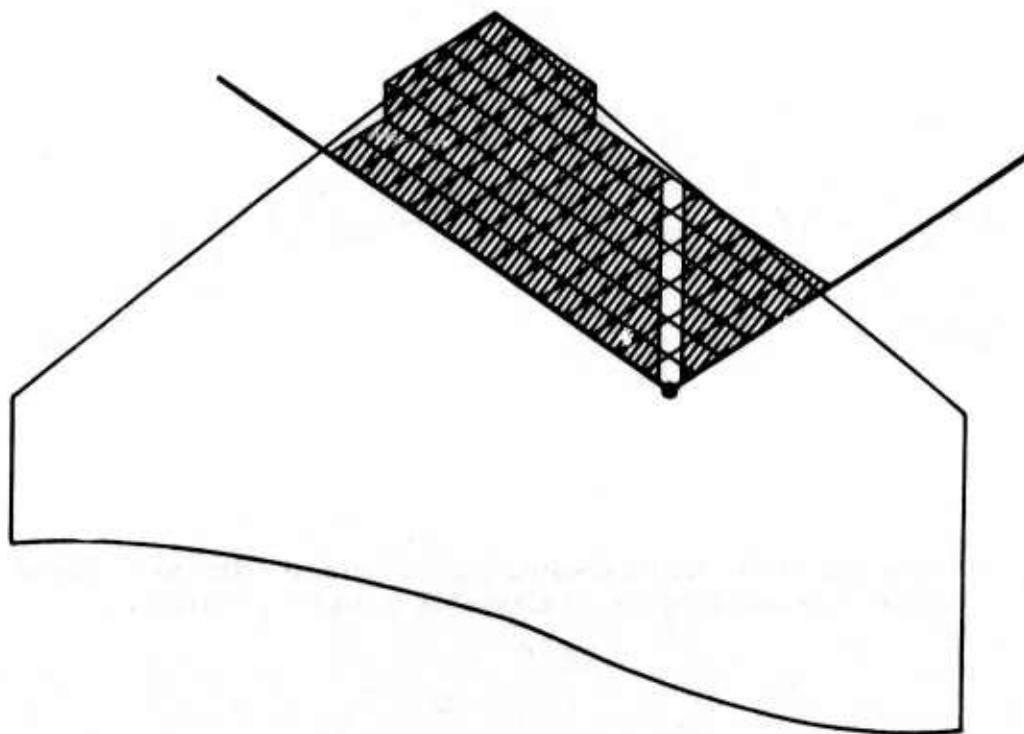


Fig. 7 - Regions of Integration for Present Method

Table 1  
 COMPARISON OF THE TWO VERSIONS OF  
 KERNEL SUBROUTINE

$M = 1.2$

$x_0 = 0.1$

$y_0 = 0.1$

Reduced Frequency, k	Modified Kernel, $\bar{K} = y_0^2 K/2$	
	Herbert Cunningham (Ref. 26)	Atlee Cunningham (Ref. 12)
0.0	(-1.3363, 0.)	(-1.3363, 0.)
0.1	(-1.3359, .026725)	(-1.3361, .019948)
1.0	(-1.2969, .26184)	(-1.3116, .19596)

Table 2  
SUMMARY OF DEMONSTRATION CASES

Planform	Mach Number, M	Leading Edge	Trailing Edge	Reduced Freq., k	Mode of Oscillation $f_i(x, y)$																								
Rectangular A = 2	1.2	Supersonic	Supersonic	0, .3, .6, 1	$1, x, x^2, y, x^2 y, xy$																								
	2.0	Supersonic	Supersonic			Arrowhead A = 4	1.12	Subsonic	Sonic	0, .5, 1	$1, x, x^2, y, y, xy$	1.25	Subsonic	Supersonic	1.5621	Subsonic	Supersonic	2.0	Supersonic	Supersonic	Tapered Swept Back A = 1.45	1.04	Subsonic	Subsonic	0, .5, 1	$1, x, x^2, y, y, xy$	1.2	Subsonic	Supersonic
Arrowhead A = 4	1.12	Subsonic	Sonic	0, .5, 1	$1, x, x^2, y, y, xy$																								
	1.25	Subsonic	Supersonic																										
	1.5621	Subsonic	Supersonic																										
	2.0	Supersonic	Supersonic																										
Tapered Swept Back A = 1.45	1.04	Subsonic	Subsonic	0, .5, 1	$1, x, x^2, y, y, xy$																								
	1.2	Subsonic	Supersonic																										
	2.0	Supersonic	Supersonic																										

Table 3  
COMPUTER PROGRAM STATISTICS FOR RECTANGULAR A = 2

Rectangular A = 2									
M	1.2			2.0					
No. of Nodes	413			368					
No. of Elements	412			367					
Program Size	25,084 <sub>10</sub>			23,832 <sub>10</sub>					
Reduced Frequency	0.0	0.3	0.6	1.0	0.0	0.3	0.6	1.0	
Execution Time (sec)	263	1276	1264	1187	130	642	703	680	

Table 4  
 COMPUTER PROGRAM STATISTICS FOR ARROWHEAD A = 4

Arrowhead A = 4												
M	1.12		1.25		1.5621		2.0					
No. of Nodes	263		441		431		527					
No. of Elements	422		400		386		480					
Program Size	26,435 <sub>10</sub>		25,273 <sub>10</sub>		24,188 <sub>10</sub>		26,523 <sub>10</sub>					
Reduced Frequency	0.0	0.5	1.0	0.0	0.5	1.0	0.0	0.5	1.0			
Execution Time	280	1466	1407	182	972	885	69	273	275	66	291	280

Table 5  
 COMPUTER PROGRAM STATISTICS FOR TAPERED SWEPTBACK A = 1.45

Tapered Swept Back A = 1.45									
M	1.04		1.2		2.0				
No. of Nodes	533		725		583				
No. of Elements	512		696		564				
Program Size	28,842 <sub>10</sub>		31,538 <sub>10</sub>		28,027 <sub>10</sub>				
Reduced Frequency	0.0	0.5	1.0	0.0	0.5	1.0	0.0	0.5	1.0
Execution Time (sec)	295	1507	1638	239	1008	1022	183	879	872

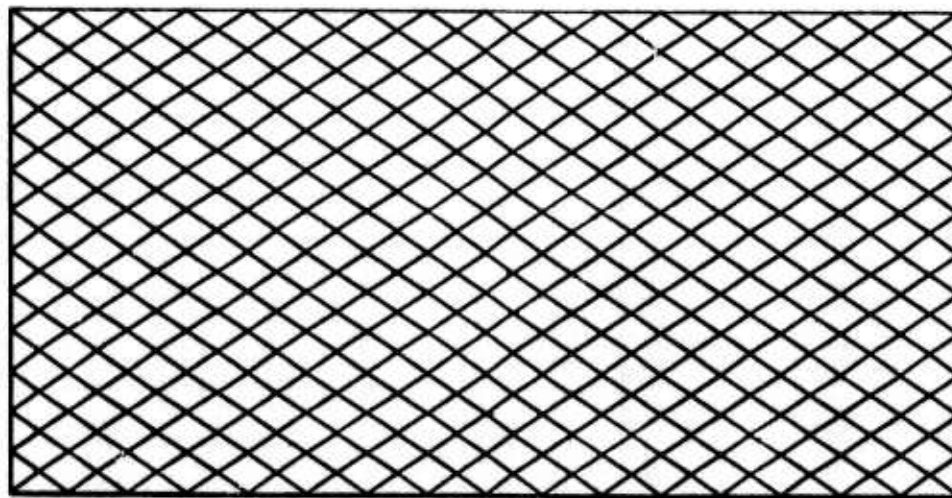


Fig. 8 - Mesh Used for Rectangular  $A = 2.0$ ,  $M = 1.2$



TABLE 7

RECTANGULAR A=2.0, M=1.2, K=0.3, DELTA=0.075, MODES= 1. X, XOX, Y+Y, XOX+Y+Y, Y, XY

	J = 1	J = 2	J = 3	J = 4	J = 5	J = 6	J = 7
1	9.3289-02	3.7051+00	2.2838-01	1.9072-02	4.4826-02	-1.8304-05	-5.0493-04
2	1.1342-03	-3.8379-01	9.9058-01	4.6638-04	2.4716-01	-7.6813-06	-2.0332-04
3	4.1851-03	3.0978-01	-4.3508-03	1.2261-03	-1.5486-02	-3.3296-06	-8.6719-05
4	1.5669-02	8.4027-01	8.7044-02	-3.2875-03	6.8599-02	-2.5047-09	2.5485-07
5	9.6397-04	8.3027-02	-1.2722-02	-1.4893-05	-1.3892-02	-5.9117-10	4.9031-07
6	3.7744-11	1.9500-09	-2.0373-10	-4.0927-12	0.0000	-2.6002-02	4.0731-01
7	-3.0777-09	-4.1560-08	3.2295-07	-3.1129-09	2.4938-07	-1.1189-02	-2.0492-01
	J = 1	J = 2	J = 3	J = 4	J = 5	J = 6	J = 7
1	3.7344+00	-9.2786-01	8.9580-01	8.8742-01	2.4842-01	-5.1364-04	4.5250-04
2	-3.8800-01	4.8397-01	-1.7350-01	-1.2113-01	-2.4110-02	-2.0698-04	1.8574-04
3	3.1023-01	-4.8731-02	5.9937-02	8.6025-02	2.6306-02	-8.8308-05	7.9654-05
4	8.4636-01	-1.3172-01	2.0032-01	2.4865-01	3.8021-02	2.4653-07	-4.9217-07
5	8.3342-02	-1.7127-02	2.2736-02	3.6086-02	1.3600-02	4.8864-07	-4.6076-07
6	4.3656-10	-1.0429-09	8.1248-10	4.5172-10	1.6977-10	3.9932-01	4.3532-01
7	-4.1103-08	1.9534-07	-7.3366-09	-1.0443-07	-3.3851-08	-2.0884-01	2.5886-01

TABLE 8

RECTANGULAR A=2., M=1.2, K=.6, DELTA=.075, MODES= 1, X, X6X, Y6Y, X6X6Y6Y, Y, XY

I	J = 1	J = 2	J = 3	J = 4	J = 5	J = 6	J = 7
1	2.6570-01	3.4020+00	4.0506-01	5.0082-02	9.1855-02	-7.3939-05	-4.7100-04
2	-2.4024-02	-4.0289-01	9.9298-01	-6.3140-03	2.5087-01	-3.1034-05	-1.0000-04
3	6.1486-03	2.9561-01	6.4710-04	2.1917-03	-1.2823-02	-1.3434-05	-6.0403-05
4	3.0408-02	7.7600-01	1.2578-01	-1.7023-02	7.3601-02	-1.0790-08	2.7462-07
5	1.3612-03	7.8846-02	-1.0769-02	-5.7987-04	-1.3053-02	1.4243-09	4.9576-07
6	-2.5466-11	2.4738-09	-1.3679-09	2.9104-11	-2.0373-10	-1.0151-01	4.6237-01
7	-1.5116-08	-3.2036-08	3.1017-07	-1.3487-08	2.4625-07	-4.2414-02	-1.7790-01

I	J = 1	J = 2	J = 3	J = 4	J = 5	J = 6	J = 7
1	3.4813+00	-5.4971-01	6.5274-01	8.2654-01	1.8624-01	-5.0633-04	4.5130-04
2	-4.2881-01	5.7017-01	-2.2607-01	-1.3229-01	-3.8760-02	-2.0370-04	1.8506-04
3	2.9413-01	-1.6320-02	4.0539-02	8.1415-02	2.0715-02	-8.6839-05	7.9321-05
4	7.9175-01	-4.6548-02	1.4507-01	2.4216-01	2.7413-02	2.3835-07	-4.8652-07
5	7.9302-02	-9.2233-03	1.7891-02	3.5323-02	1.2423-02	4.9098-07	-4.6958-07
6	8.3674-10	-5.8208-10	-2.4253-11	5.0325-10	6.0633-11	4.3237-01	4.1361-01
7	-2.7949-08	1.9575-07	6.3058-10	-1.0122-07	-3.2918-08	-1.9231-01	2.4524-01

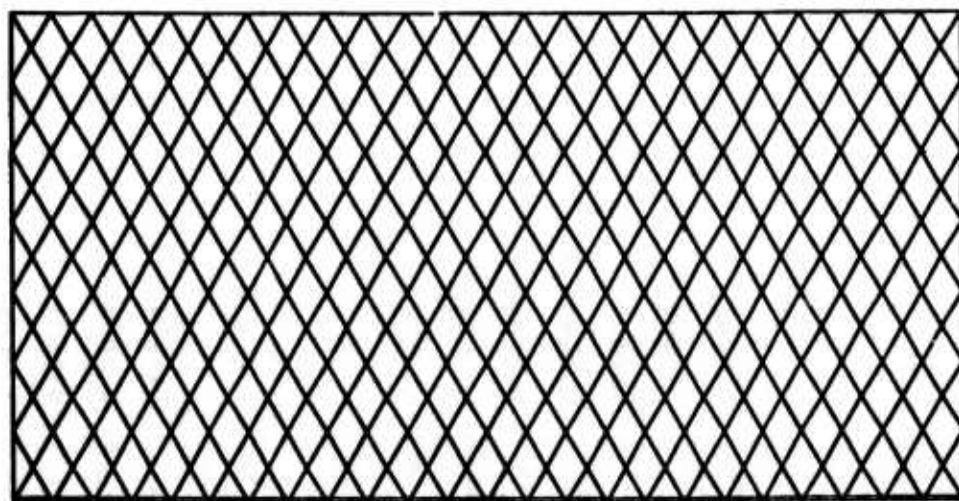
TABLE 9

RECTANGULAR A=2.0, M=1.2, K=1.0, DELTA=.075, MODES= 1, X, XOX, YOY, XOXOYOY, Y, XY

I	J = 1	J = 2	J = 3	J = 4	J = 5	J = 6	J = 7
1	3.6016-01	3.1489+00	3.1703-01	4.6815-02	1.2581-01	-2.0914-04	-3.8577-04
2	-1.4517-01	-3.2979-01	9.2296-01	-3.5214-02	2.3960-01	-8.7538-05	-1.5270-04
3	-1.0602-02	3.0485-01	-1.4367-02	-1.4308-03	-1.3837-02	-3.7900-05	-6.4613-05
4	2.2160-02	7.2894-01	1.4788-01	-6.3747-02	7.1690-02	-5.0815-08	3.3266-07
5	-2.9836-03	7.9095-02	-1.2579-02	-2.9648-03	-1.2462-02	1.0441-08	4.9272-07
6	2.9104-11	5.5297-10	-6.4028-10	3.2742-11	2.1828-10	-2.5200-01	5.7698-01
7	-1.4406-08	-2.0751-08	2.9757-07	-3.1754-08	2.4150-07	-1.0011-01	-1.2659-01

I	J = 1	J = 2	J = 3	J = 4	J = 5	J = 6	J = 7
1	3.2508+00	-1.1758-01	3.9409-01	7.7198-01	1.1784-01	-4.8607-04	4.4587-04
2	-4.1922-01	6.2888-01	-2.5158-01	-1.3249-01	-4.8504-02	-1.9471-04	1.8238-04
3	2.9508-01	5.5548-03	3.1792-02	8.0277-02	1.6938-02	-8.2843-05	7.8079-05
4	7.4586-01	4.9528-02	8.6586-02	2.4369-01	1.7935-02	2.1892-07	-4.5940-07
5	7.8780-02	-3.1786-03	1.5022-02	3.5355-02	1.1486-02	4.7855-07	-4.6573-07
6	1.5134-09	-3.7835-10	6.4756-10	4.4565-10	2.7649-10	5.1055-01	3.5192-01
7	1.0543-08	1.5472-07	4.1149-04	-8.9562-08	-2.3661-08	-1.5781-01	2.1335-01



**Fig. 9 - Mesh Used for Rectangular  $A = 2.0$ ,  $M = 2.0$**



TABLE 11

RECTANGULAR A=2.0, M=2.0, K=3.0, DELTA=0.833, MODES= 1, X, XOX, YOY, XOXYOY, Y, XY

I	J = 1	J = 2	J = 3	J = 4	J = 5	J = 6	J = 7
1	3.5686-03	2.0063+00	-2.5984-01	-9.7554-04	-4.4248-02	-9.5222-08	-2.3641-06
2	2.0666-04	-4.2445-02	3.6551-01	-5.1926-04	1.1786-01	-3.7626-08	-8.3500-07
3	1.8045-04	1.7090-01	-1.7093-02	-1.6483-04	-4.8265-03	-7.9663-09	-1.7150-07
4	-1.2390-03	5.1765-01	-3.6377-02	-2.2950-03	7.8966-03	2.6776-09	1.7272-07
5	-1.9281-04	4.5276-02	-4.1905-03	-2.8134-04	-1.5494-03	4.8956-09	3.0506-07
6	4.5475-13	7.2760-11	4.0745-10	1.8190-12	-6.7311-11	-2.5323-03	4.7413-01
7	-1.6259-09	-3.0395-08	3.5363-07	-1.7794-09	1.7273-07	-1.0164-03	-4.6906-02

I	J = 1	J = 2	J = 3	J = 4	J = 5	J = 6	J = 7
1	2.0190+00	-1.7181-01	4.3499-01	5.2807-01	1.0644-01	-2.4069-06	2.1976-06
2	-4.0032-02	1.8031-01	2.2874-02	-3.4441-02	2.4380-04	-8.5268-07	8.2198-07
3	1.7200-01	-1.0644-02	4.7002-02	4.6121-02	1.2273-02	-1.8008-07	-5.3342-06
4	5.2046-01	-4.8689-03	1.0171-01	2.2165-01	3.4642-02	1.7180-07	-1.8961-07
5	4.5505-02	3.4880-05	1.1822-02	2.0166-02	4.6956-03	3.0382-07	-4.3610-07
6	9.8225-10	-1.2127-10	1.2733-10	4.0169-11	-5.4570-11	4.7637-01	2.1903-02
7	-2.8464-08	1.9515-07	1.2812-08	-4.4152-08	-1.3242-08	-4.6635-02	7.3410-02

TABLE 12

RECTANGULAR A=2.0, M=2.0, K=6.0, DELTA=0.033, MODES= 1. X, XOX, YOY, KXOXOY, Y, XY

	J = 1	J = 2	J = 3	J = 4	J = 5	J = 6	J = 7
1	1.4317-02	1.9672+00	-2.3701-01	-3.8566-03	-3.9406-02	-3.7555-07	-2.1527-06
2	6.4120-04	-1.9949-02	3.6957-01	-2.0617-03	1.1849-01	-1.4820-07	-7.5082-07
3	7.2776-04	1.6753-01	-1.5197-02	-6.5321-04	-4.4817-03	-3.0906-08	-1.3381-07
4	-4.9056-03	5.0973-01	-3.1838-02	-9.1135-03	8.6325-03	1.0690-08	1.7340-07
5	-7.6435-04	4.4678-02	-3.8819-03	-1.1161-03	-1.5789-03	1.9692-08	3.0959-07
6	5.4570-12	-8.3674-10	-5.8208-11	-1.6371-11	4.3656-11	-1.0026-02	4.6869-01
7	-6.4556-09	-3.3939-08	3.5540-07	-7.0522-09	1.7291-07	-4.0287-03	-4.7237-02

	J = 1	J = 2	J = 3	J = 4	J = 5	J = 6	J = 7
1	2.0179+00	-1.6720-01	4.3192-01	5.2850-01	1.0583-01	-2.3306-06	2.1471-06
2	-4.0307-02	1.6188-01	2.1847-02	-3.4272-02	4.1338-05	-8.2056-07	8.0017-07
3	1.7190-01	-1.0068-02	4.6614-02	4.6191-02	1.2199-02	-1.6804-07	-6.2713-08
4	5.2101-01	-4.0840-03	1.0114-01	2.2268-01	3.4639-02	1.7158-07	-1.8949-07
5	4.5591-02	1.3385-04	1.1754-02	2.0310-02	4.6999-03	3.0424-07	-4.3638-07
6	-1.5158-10	4.9719-10	-1.5158-10	4.3201+10	9.0949-11	4.7769-01	2.2164-02
7	-2.8570-08	1.9718-07	1.1775-08	-4.3461-08	-1.3406-08	-4.6141-02	7.3486-02

TABLE 13

RECTANGULAR A=2., M=2., K=1., DELTA=.0833, MODES= 1. X, X^2, Y, Y^2, X\*Y, X\*Y^2, Y, XY

	J = 1	J = 2	J = 3	J = 4	J = 5	J = 6	J = 7
1	4.0155-02	1.8746+00	-1.8309-01	-1.0389-02	-2.7907-02	-1.0089-06	-1.6758-06
2	2.4709-03	-6.7640-02	3.7909-01	-5.6172-03	1.1996-01	-3.9687-07	-5.5946-07
3	2.0763-03	1.5958-01	-1.0744-02	-1.7706-03	-3.6656-03	-7.9735-08	-4.8419-08
4	-1.3271-02	4.9087-01	-2.1048-02	-2.4874-02	1.0488-02	2.9482-08	1.7447-07
5	-2.0745-03	4.3251-02	-3.1498-03	-3.0368-03	-1.6348-03	5.5372-08	3.1971-07
6	-1.4552-11	1.1205-09	4.0745-10	7.2760-12	-4.3656-11	-2.7162-02	4.5950-01
7	-1.7564-08	-4.1418-08	3.5917-07	-1.9358-08	1.7247-07	-1.0944-02	-4.8122-02

	J = 1	J = 2	J = 3	J = 4	J = 5	J = 6	J = 7
1	2.0153+00	-1.5640-01	4.2473-01	5.2951-01	1.0440-01	-2.1533-06	2.0293-06
2	-4.0715-02	1.8554-01	1.9440-02	-3.3871-02	-4.3487-04	-7.4725-07	7.5117-07
3	1.7168-01	-8.6698-03	4.5704-02	4.6355-02	1.2023-02	-1.4016-07	-8.4048-08
4	5.2231-01	-2.2343-03	9.9813-02	2.2508-01	3.4620-02	1.7038-07	-1.8979-07
5	4.5775-02	3.6760-04	1.1592-02	2.0644-02	4.7080-03	3.0513-07	-4.3678-07
6	6.1118-10	-1.6007-10	-2.6193-10	6.6393-10	-7.2760-12	4.8078-01	2.2811-02
7	-2.6837-06	2.0123-07	9.0586-09	-4.2011-08	-1.3762-08	-4.4996-02	7.3679-02

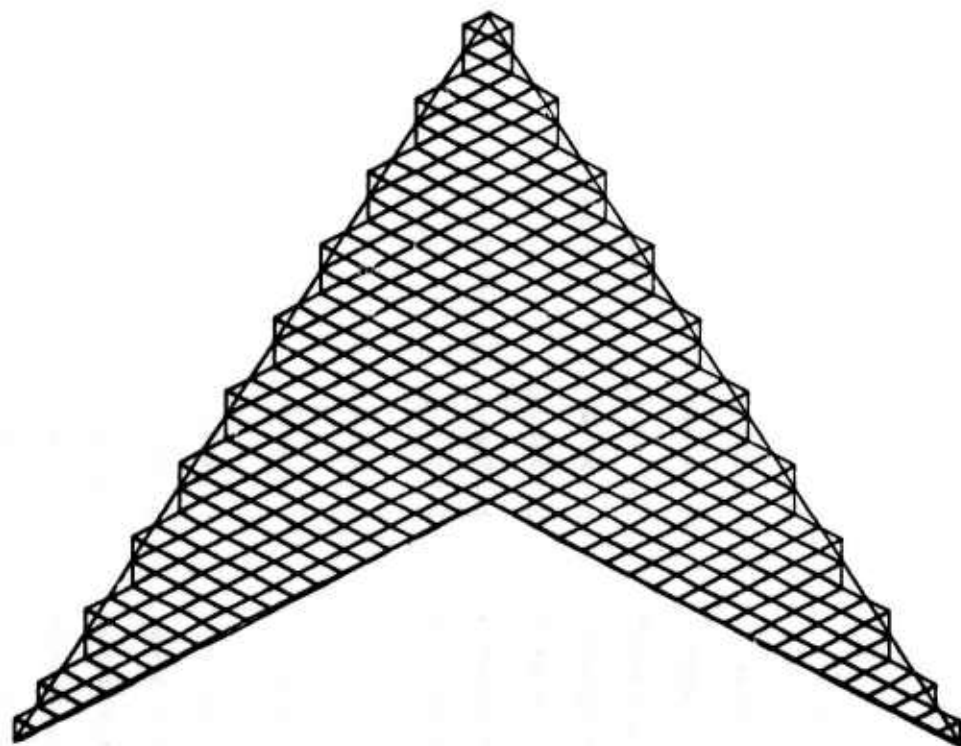


Fig. 10 - Mesh Used for Arrowhead  $A = 4.0$ ,  $M = 1.12$

Table 14

ARRONHEAD A=4.0 M=1.12. K=0.0. DELTA=.056. MODES= 1, X, XAX, Y, Y, Y, XY

I	J = 1	J = 2	J = 3	J = 4	J = 5	J = 6
1	0.0000	2.1982+00	2.1512+00	0.0000	0.0000	7.7918+04
2	0.0000	7.6935-01	1.2195+00	0.0000	0.0000	3.2313+04
3	0.0000	5.1177-01	7.3115-01	0.0000	0.0000	1.3717+04
4	0.0000	4.8900-01	6.2936-01	0.0000	0.0000	1.4457+06
5	0.0000	2.3283-10	2.3263-10	0.0000	0.0000	3.2075+01
6	0.0000	-8.6671-08	4.7090-08	0.0000	0.0000	1.9694+01

I	J = 1	J = 2	J = 3	J = 4	J = 5	J = 6
1	0.0000	0.0000	0.0000	0.0000	0.0000	0.0000
2	0.0000	0.0000	0.0000	0.0000	0.0000	0.0000
3	0.0000	0.0000	0.0000	0.0000	0.0000	0.0000
4	0.0000	0.0000	0.0000	0.0000	0.0000	0.0000
5	0.0000	0.0000	0.0000	0.0000	0.0000	0.0000
6	0.0000	0.0000	0.0000	0.0000	0.0000	0.0000

Table 15

ARRONHEAD A4400 M=1.12, K=0.8, DELTA=0.056, MODES = 1, X, KX1, Y, Y, XY

	J = 1	J = 2	J = 3	J = 4	J = 5	J = 6
1	4.2057-02	2.1742+00	2.0685+00	1.7999+02	1.3979+04	6.5708+04
2	2.6166-02	7.5887+01	1.1706+00	9.7768+03	5.8350+05	2.7199+04
3	1.9132-02	5.0524+01	6.9924+01	6.2650+03	2.9830+05	8.1536+04
4	2.8006-02	4.8095+01	6.0391+01	5.2041+03	1.0531+07	1.3317+06
5	0.0000	0.0000	0.0000	0.0000	-3.4393+03	3.2249+01
6	3.2688-08	-9.9244+08	2.9861+08	5.1696+07	-1.5328+03	1.9815+01

	J = 1	J = 2	J = 3	J = 4	J = 5	J = 6
1	2.4170+00	8.5785-01	7.8210+02	4.5564+01	7.1755+04	-9.1948+04
2	7.2718+01	4.7459+01	8.1703+02	2.5239+01	2.9727+04	-3.8278+04
3	4.8474+01	2.6881+01	6.8504+02	1.7110+01	1.2613+04	-1.6248+04
4	4.6393+01	2.0664+01	5.8136+02	1.6952+01	1.3966+06	-4.9177+07
5	4.6566+10	5.8208+11	1.1642+10	0.0000	3.2122+01	2.5003+01
6	-1.1275+07	-1.2186+07	-1.6767+07	-1.2055+07	1.9715+01	1.6926+01

Table 16

ARROWHEAD A=4.0 M=1.12 K=1.0 DELTA=0.56. MODES 1. X. X0X. Y0Y. Y. XY

I	J = 1	J = 2	J = 3	J = 4	J = 5	J = 6
1	7.1059+02	2.2384+00	1.9483+00	4.7529+02	4.9696+04	3.3761+04
2	6.0408+02	7.9112+01	1.1097+00	2.4793+02	2.0736+04	1.3826+04
3	4.9605+02	5.2310+01	6.6196+01	1.5695+02	8.8191+05	5.8337+05
4	6.6249+02	4.8923+01	5.7197+01	1.3279+02	3.7169+07	1.0297+06
5	0.0000	2.3283+10	0.0000	0.0000	-1.4120+02	3.2808+01
6	1.0553+07	-1.0611+07	4.2492+09	1.5192+08	-6.3833+03	2.0200+01

63

I	J = 1	J = 2	J = 3	J = 4	J = 5	J = 6
1	2.0886+00	8.7905+01	2.0976+01	4.3302+01	5.5666+04	-7.9344+04
2	7.1257+01	4.7682+01	1.5947+01	2.3972+01	2.2977+04	-3.2983+04
3	4.7249+01	2.6910+01	1.1824+01	1.6290+01	9.7307+05	-1.3984+04
4	4.8564+01	2.1027+01	9.7437+02	1.6262+01	1.2635+06	-3.2820+07
5	2.3283+10	5.8208+11	1.1642+10	1.1642+10	3.2434+01	2.4929+01
6	-1.4313+07	-1.0998+07	-1.4112+07	-1.2654+07	1.9892+01	1.6868+01

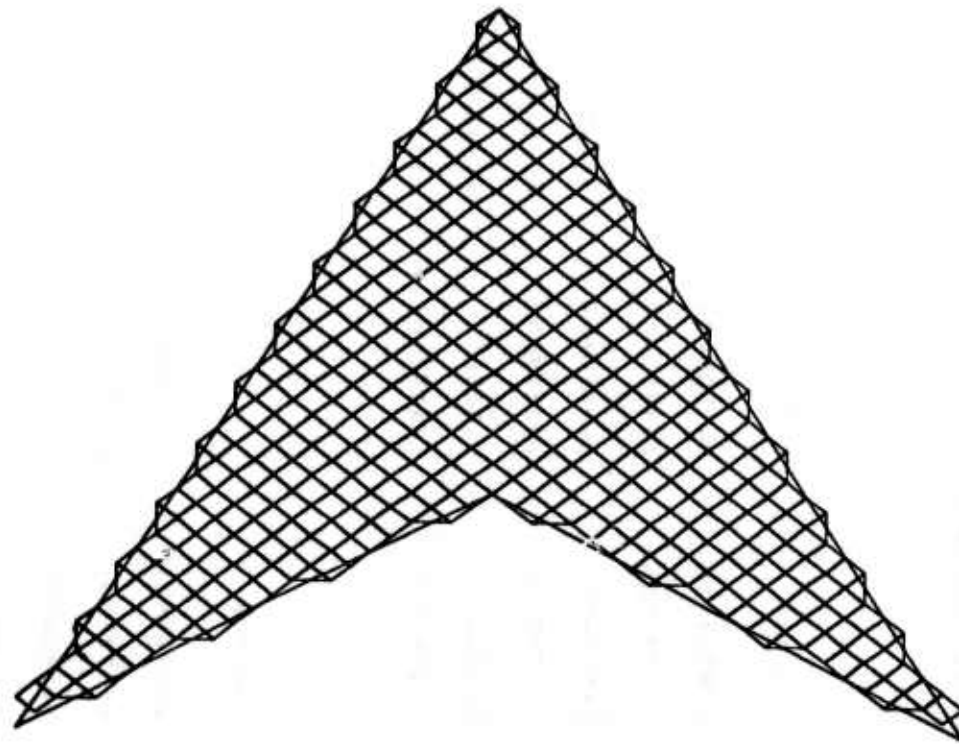


Fig. 11 - Mesh Used for Arrowhead  $A = 4.0$ ,  $M = 1.25$

Table 17

ARROWHEAD A=7.0, M=1.05, K=0.0, DELTA=0.520833333, MODES= 1, X, XOX, Y, Y, XY

	J = 1	J = 2	J = 3	J = 4	J = 5	J = 6
1	0.0000	1.9413+00	1.7231+00	0.0000	0.0000	3.6727-05
2	0.0000	7.3782-01	1.0136+00	0.0000	0.0000	1.6162-05
3	0.0000	4.8753-01	6.2635-01	0.0000	0.0000	7.3451-06
4	0.0000	4.5595-01	5.1280-01	0.0000	0.0000	2.4452-07
5	0.0000	1.7462-10	-5.8208-11	0.0000	0.0000	2.9368-01
6	0.0000	7.6863-02	6.8801-08	0.0000	0.0000	1.8460-01
1	0.0000	0.0000	0.0000	0.0000	0.0000	0.0000
2	0.0000	0.0000	0.0000	0.0000	0.0000	0.0000
3	0.0000	0.0000	0.0000	0.0000	0.0000	0.0000
4	0.0000	0.0000	0.0000	0.0000	0.0000	0.0000
5	0.0000	0.0000	0.0000	0.0000	0.0000	0.0000
6	0.0000	0.0000	0.0000	0.0000	0.0000	0.0000

Table 18

ARROWHEAD A4.0, M=1.25, K=0.5, DELTA=0.52083333, MODES= I, X, XOX, YOY, Y, XY

I	J = 1	J = 2	J = 3	J = 4	J = 5	J = 6
1	4.6968202	1.927200	1.702800	9.041403	5.431306	3.278208
2	3.087302	7.303301	1.000400	5.422703	2.422606	1.438905
3	2.2946202	4.822601	6.173301	3.749703	1.100206	6.530506
4	2.615202	4.492601	5.061201	3.302303	2.002709	2.474707
5	1.455211	-5.238710	0.0000	0.0000	4.264504	2.953301
6	1.608008	7.150808	6.903408	1.316909	9.100604	1.858901

66

I	J = 1	J = 2	J = 3	J = 4	J = 5	J = 6
1	1.903600	6.636401	2.174101	3.586501	3.545705	-4.114805
2	7.148901	3.761201	1.421801	2.087201	1.558405	-1.822805
3	4.714001	2.161801	1.021301	1.445901	7.078706	-8.276406
4	4.404901	1.477801	8.351702	1.411101	2.467707	1.284107
5	9.895310	1.018610	-2.910411	-1.164210	2.935601	2.038001
6	7.046008	3.021008	5.064109	-6.883109	1.844101	1.407001

Table 19

ARROWHEAD A400 MP1.25 . K=1.0 DELTA=0.0520833333, MODES= 1, X, XOX, YOY, Y, XY

	J = 1	J = 2	J = 3	J = 4	J = 5	J = 6
1	1.2954+01	1.9276+00	1.6463+00	3.0393+02	1.9712+05	1.9213+05
2	8.9370+02	7.6320+01	9.6586+01	1.7899+02	8.7832+06	8.3225+06
3	6.8726+02	4.8229+01	5.9446+01	1.2320+02	3.9842+06	3.7524+06
4	8.4261+02	4.4229+01	4.8707+01	1.1056+02	5.9808+09	2.4351+07
5	-5.8208-11	1.7462+10	-2.9104+10	7.2760+12	1.3676+03	3.0003+01
6	5.7742+08	5.9401+08	6.9267+08	4.7730+09	3.3675+03	1.8954+01

	J = 1	J = 2	J = 3	J = 4	J = 5	J = 6
1	1.8455+00	6.9393+01	2.4129+01	3.4845+01	2.9335+05	-3.6847+05
2	6.7949+01	3.9116+01	1.5951+01	2.0230+01	1.2839+05	-1.6156+05
3	4.4570+01	2.2575+01	1.1460+01	1.4011+01	5.8224+06	-7.3236+06
4	4.1228+01	1.5765+01	9.2710+02	1.3733+01	2.4078+07	1.3050+07
5	4.0745+10	3.6380+10	0.0000	0.0000	2.9373+01	2.0252+01
6	5.7771+08	-2.4067+08	5.7335+09	-7.6980+09	1.8422+01	1.3967+01

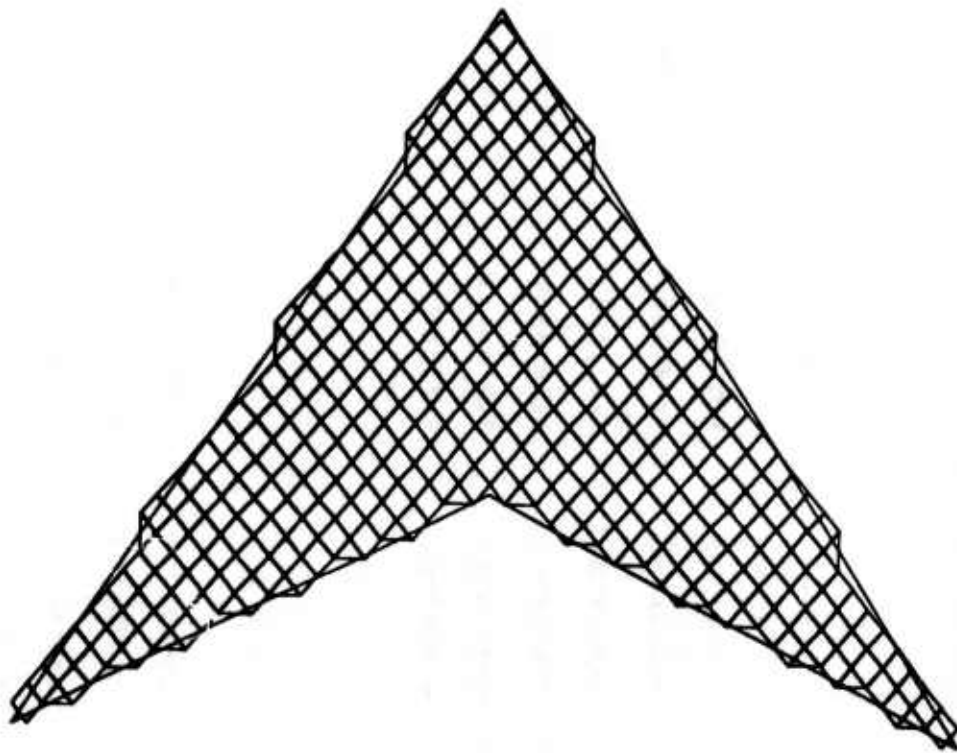


Fig. 12 - Mesh Used for Arrowhead  $A = 4.0$ ,  $M = 1.5621$



Table 21

ARROWHEAD A=4., M=1.5621, K=5., DELTA=.05207, MODES 1., X., Xax, Yax, Y., XY

	J = 1	J = 2	J = 3	J = 4	J = 5	J = 6
1	1.0296-02	1.2970+00	1.0201+00	2.1594-03	7.5927-06	1.5696-03
2	1.0226-02	4.9526-01	6.1141-01	1.5172-03	-1.2452-06	-4.3150-04
3	8.8897-03	3.2627-01	3.8310-01	1.2027-03	3.3805-07	1.1938-04
4	1.1730-02	3.1517-01	3.1388-01	1.3019-03	6.2201-08	2.7420-05
5	9.7374-06	1.8293-03	-1.0887-03	3.0077-08	2.7182-03	2.4764-01
6	-2.6896-06	-5.0188-04	2.9970-04	-7.8444-09	2.2251-03	:.5798-01
70						
1	J = 1	J = 2	J = 3	J = 4	J = 5	J = 6
1	1.3016+00	4.7003-01	2.9340-01	2.5144+01	1.5722+03	-4.8151-04
2	4.9695-01	2.6538-01	1.8572-01	1.5388-01	-4.3222-04	1.3296-04
3	3.2706-01	1.5623-01	1.3163-01	1.1031-01	1.1957-04	-3.6933-05
4	3.1579-01	1.0995-01	1.1117-01	1.0983-01	2.9451-05	-8.3472-04
5	1.8342-03	-5.8443-04	2.0328-04	3.2398-05	2.4751-01	1.4009-01
6	-5.0318-04	1.6059-04	-5.5803-05	-8.8222-06	1.5770-01	9.9538-02

Table 22

ARROWHEAD A=4.0 M=1.5621. K=1.0. DELTA=0.05207. MODES= 1. X. XOX. Y.Y. Y. XY

	J = 1	J = 2	J = 3	J = 4	J = 5	J = 6
1	3.4367+02	1.2709+00	1.0216+00	0.3401+03	1.0360+05	1.5615+03
2	3.6072+02	4.7973+01	6.1257+01	5.0462+03	-4.9779+06	-4.2931+04
3	3.1907+02	3.1529+01	3.0451+01	4.6361+03	1.3514+06	1.1070+04
4	4.3473+02	3.0353+01	3.1600+01	5.0475+03	2.4024+07	2.9322+05
5	3.0001+05	1.0130+03	-1.0814+03	1.2014+07	1.0371+02	2.4612+01
6	-1.0421+05	-4.9771+04	2.7772+04	-3.1350+08	0.4985+03	1.5725+01

	J = 1	J = 2	J = 3	J = 4	J = 5	J = 6
1	1.2070+00	4.0137+01	7.9011+01	2.5026+01	1.5721+03	-4.0149+04
2	4.0563+01	2.7266+01	1.0360+01	1.5299+01	-4.3216+04	1.3296+04
3	3.4703+01	1.6140+01	1.3015+01	1.0960+01	1.1956+04	-3.6932+05
4	3.0544+01	1.1476+01	1.0955+01	1.0911+01	2.9446+05	-0.3466+06
5	1.0332+03	-5.0404+04	2.0310+04	3.2395+05	2.4564+01	1.4055+01
6	-5.0293+04	1.6040+04	-5.5757+05	-0.0213+06	1.5610+01	9.9045+02

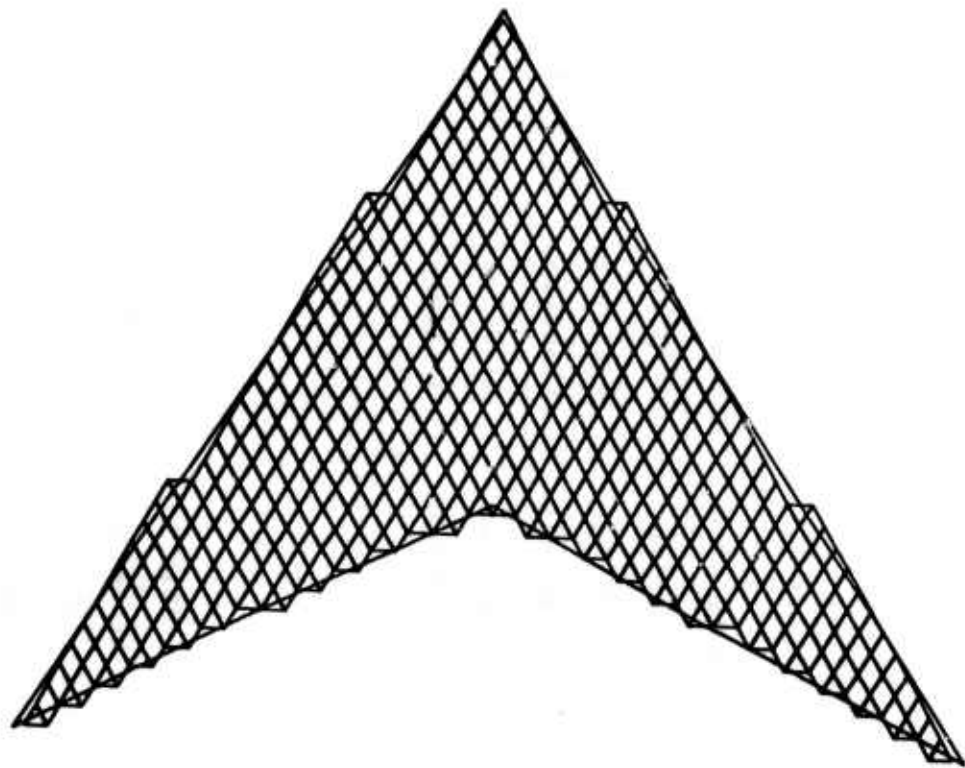


Fig. 13 - Mesh Used for Arrowhead  $A = 4.0$ ,  $M = 2.0$



Table 24

ARRONMEAD A=4.0, M=2.0, K=0.5, DELTA=0.95, MODES= 1, X, XOX, Y, Y, XY

	J = 1	J = 2	J = 3	J = 4	J = 5	J = 6
1	4.5947-02	1.2816+00	8.5078-01	5.7222-03	3.0241-10	-4.6566-10
2	2.3193-02	4.6742-01	5.3826-01	3.6288-03	1.3188-10	-4.3656-11
3	1.5401-02	3.1031-01	3.3190-01	2.5916-03	2.5193-10	-1.5527-08
4	1.4006-02	2.8773-01	2.7625-01	2.3316-03	5.7616-10	-4.5860-08
5	1.5461-11	-4.3656-10	-5.2387-10	1.3642-12	6.6315-03	2.4292-01
6	-6.7394-10	-1.1540-08	-1.0637-08	-2.7285-10	4.4943-03	1.5137-01
1	1.2672+00	2.4147-01	2.5361-01	2.4429-01	-8.1491-10	-7.5670-10
2	4.6795-01	1.7631-01	1.4575-01	1.4731-01	-1.0166-10	-3.4197-10
3	3.1017-01	1.0413-01	1.0472-01	1.0496-01	-1.5498-08	-1.6254-08
4	2.6744-01	8.1666-02	7.0750-02	1.0464-01	-4.6501-08	-4.8421-08
5	7.6560-10	1.1642-10	1.5280-10	-1.0166-10	2.4172-01	1.1121-01
6	-1.0699-08	-2.6412-09	-4.6639-09	4.5111-10	1.9032-01	8.0398-02

Table 25

ARROWHEAD A=4.7 M=2.7 K=1.7 DELTA=0.5, MODES= 1, X, XOX, Y=Y, Y, XY

	J = 1	J = 2	J = 3	J = 4	J = 5	J = 6
1	1.7715-01	1.2316+00	8.6708-01	2.2656-02	2.3774+09	1.9791-09
2	8.8506-02	4.4699-01	5.4548-01	1.4346-02	1.0441-09	9.4587-10
3	5.8668-02	2.9841-01	3.3695-01	1.0238-02	1.1478-09	-1.4683-08
4	5.3742-02	2.7897-01	2.8133-01	9.2188-03	2.1282-09	-4.5482-08
5	1.0914-10	5.8208-11	8.1491-10	2.7285-11	2.6076-02	2.4344-01
6	-2.0482-09	-1.0696-08	-1.0579-08	-1.0514-09	1.7634-02	1.5235-01

75

	J = 1	J = 2	J = 3	J = 4	J = 5	J = 6
1	1.2522+20	2.5618-01	2.4790-01	2.4216-01	1.5716-09	-2.3865-09
2	4.4508-01	1.8422-01	1.4256-01	1.4891-01	1.0623-09	-1.1569-09
3	2.8721-01	1.0907-01	1.8269-01	1.8356-01	-1.5207-08	-1.6662-08
4	2.7733-01	8.5273-02	8.9156-02	1.0404-01	-4.6853-08	-4.8509-08
5	-1.1642-10	5.8208-11	9.4587-11	4.3656-11	2.3864-01	1.1156-01
6	-9.8972-09	-2.1868-09	-4.5620-09	5.6752-10	1.4814-01	8.0604-02

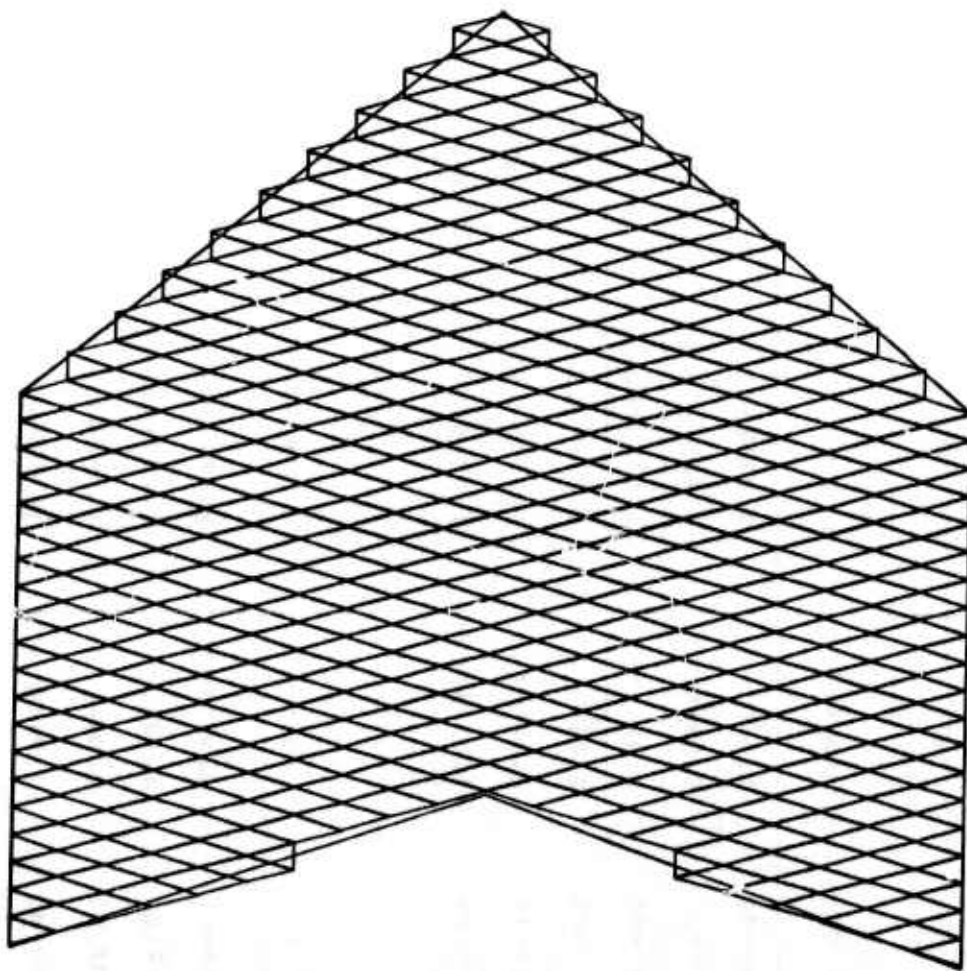


Fig. 14 - Mesh Used for Tapered Sweptback  $A = 1.45$ ,  $M = 1.04$

Table 26

TAPERED SWEPT BACK A=1.45, M=1.04, K=0., DELTA=.104, MODES=1, X. X.X, Y.Y, Y. XY

I	J = 1	J = 2	J = 3	J = 4	J = 5	J = 6
1	0.0000	3.6156+00	4.7277+00	0.0000	0.0000	-9.9691-10
2	0.0000	-1.1273+00	3.2414+00	0.0000	0.0000	-1.3824-10
3	0.0000	1.0696-01	1.2630+00	0.0000	0.0000	1.3587-06
4	0.0000	7.6271-01	1.2480+00	0.0000	0.0000	1.2946-05
5	0.0000	3.6380-10	-2.6193-10	0.0000	0.0000	4.8842-01
6	0.0000	-1.2905-06	2.3554-06	0.0000	0.0000	-7.8788-02

I	J = 1	J = 2	J = 3	J = 4	J = 5	J = 6
1	0.0000	0.0000	0.0000	0.0000	0.0000	0.0000
2	0.0000	0.0000	0.0000	0.0000	0.0000	0.0000
3	0.0000	0.0000	0.0000	0.0000	0.0000	0.0000
4	0.0000	0.0000	0.0000	0.0000	0.0000	0.0000
5	0.0000	0.0000	0.0000	0.0000	0.0000	0.0000
6	0.0000	0.0000	0.0000	0.0000	0.0000	0.0000

Table 27

TAPERED SWEEP BACK A=1.45, M=1.04, K=5, DELTA=.104, MODE=1, X, X+X, Y, Y, XY

	J = 1	J = 2	J = 3	J = 4	J = 5	J = 6
1	-4.8753-01	4.7790+00	3.9317+00	-1.2856-02	3.2742-11	-2.6557-10
2	-4.2319-01	-1.4562-01	3.1163+00	-1.0651-01	7.2760-12	-1.7462-10
3	-2.4139-01	6.4668-01	1.3380+00	-6.6341-02	1.6335-08	1.3980-06
4	-1.1999-01	1.0184+00	1.0991+00	-1.9960-02	2.0037-07	1.3428-05
5	-4.3656-11	-8.7311-11	-9.3132-10	1.3461-10	-8.4559-02	4.4244-01
6	1.7324-07	-1.5657-06	2.5258-06	1.8688-08	-3.0873-02	-1.3371-01
78						
	J = 1	J = 2	J = 3	J = 4	J = 5	J = 6
1	4.5608+20	3.8715+00	-3.5988-01	1.6729+00	-1.0914-11	-4.3656-10
2	-1.9020-21	3.2073+00	4.3423-01	1.4369-01	-1.0550-10	2.9104-11
3	6.4573-01	1.6577+00	7.3383-01	1.8946-01	1.3780-06	-6.5874-07
4	9.8333-01	1.0194+00	9.8301-02	4.5916-01	1.3184-05	-7.1181-06
5	-4.2928-10	-1.5716-09	-9.3132-10	2.2192-10	4.7451-01	6.2097-01
6	-1.4806-06	5.5236-07	4.5286-07	-9.6080-07	-1.0487-01	2.8412-01

Table 28

TAPERED SWEEP BACK A=1.45, M=1.04, K=1., DELTA=.104, MODES=1, X, XOX, YOY, Y, XY

	J = 1	J = 2	J = 3	J = 4	J = 5	J = 6
1	-8.8905-01	5.8570+00	3.2911+00	1.9131-01	1.1642-10	-2.6193-10
2	-8.1316-01	5.3779-01	2.9936+00	-9.8581-02	-1.1642-10	-3.2014-10
3	-4.8213-01	1.0572+00	1.2967+00	-6.3256-02	1.0293-07	1.4485-06
4	-2.1943-01	1.2390+00	9.6805-01	-1.3237-02	1.2607-06	1.4049-05
5	2.9104-10	8.0036-10	0.0000	1.8917-10	-3.9554-01	4.0456-01
6	5.2433-07	-1.8797-06	2.6740-06	5.5283-08	-1.9038-01	-2.3015-01
1	J = 1	J = 2	J = 3	J = 4	J = 5	J = 6
1	5.3908+00	2.5048+00	3.7539-01	1.7234+00	5.7844-10	-2.9104-11
2	4.1638-01	2.2592+00	4.5851-01	2.7782-01	-1.5280-10	-2.9104-11
3	1.0266+00	1.1035+00	6.2813-01	2.8114-01	1.3743-06	-7.1173-07
4	1.1793+00	6.9966-01	2.4086-01	4.7767-01	1.3136-05	-7.7721-06
5	-6.5484-10	-6.9849-10	-1.0477-09	-1.9645-10	5.1745-01	7.2253-01
6	-1.6010-06	7.7212-07	3.1153-07	-9.9269-07	-1.2148-01	3.8741-01

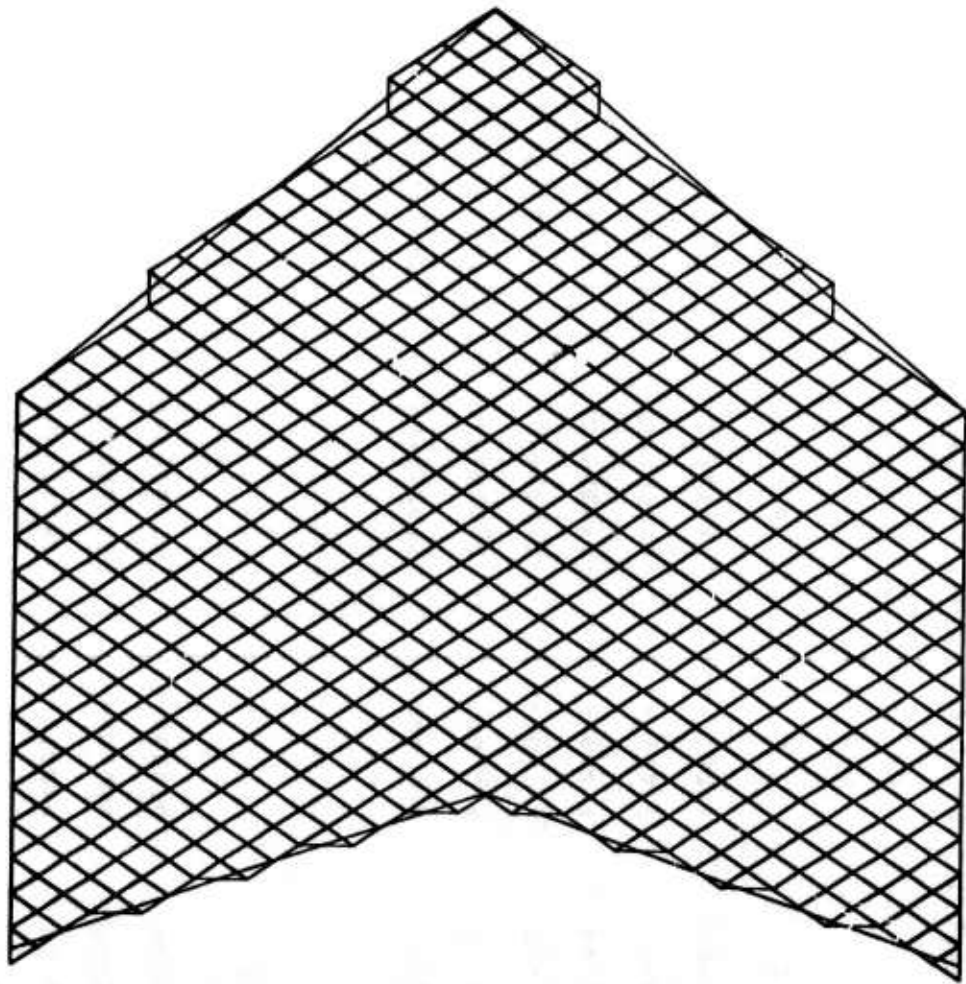


Fig. 15 - Mesh Used for Tapered Sweptback  $A = 1.45$ ,  $M = 1.2$



Table 30

TAPERED SWEPT BACK A=1.45, M=1.2, K=5, DELTA=1/15, MODES= 1, X, XOX, Y, Y, XY

	J = 1	J = 2	J = 3	J = 4	J = 5	J = 6
1	-8.5295-02	4.1089+00	3.5953+00	5.3794-02	-2.7285-10	2.2010-10
2	-1.8266-01	3.0117-01	3.0158+00	7.5656-03	1.2551-10	-1.6007-10
3	-1.3157-01	6.7078-01	1.6080+00	1.4807-03	3.5310-08	1.5153-07
4	-3.8698-02	9.4453-01	9.9862-01	-8.3241-03	5.8391-08	-3.7428-08
5	-8.5493-11	1.7644-10	5.8208-11	4.0927-12	-1.2275-01	4.2071-01
6	-1.0014-08	4.1691-08	2.2320-07	-8.1368-09	-8.8164-02	-1.1293-01

82

	J = 1	J = 2	J = 3	J = 4	J = 5	J = 6
1	3.9771+00	2.1630+00	-8.9194-03	1.1116+00	3.3970-10	1.4043-09
2	1.8547-01	2.2550+00	-2.3667-01	1.9049-01	-1.3642-10	-3.9290-10
3	5.9998-01	1.3374+00	1.1057-01	1.6166-01	1.3788-07	-2.8963-07
4	9.1907-01	6.6026-01	1.3458-01	3.2129-01	-6.5809-08	-4.9296-07
5	5.4933-10	2.7358-09	7.2760-11	-1.3279-10	4.3457-01	8.6246-01
6	4.2852-08	1.5309-07	1.2708-07	-6.8885-08	-9.6999-02	5.9657-01

Table 31

TAPERED SWEPT BACK A=1.45, M=1.2, K=1., DELTA=1/15, MODES= 1, X, XOX, Yoy, Y, XY

	J = 1	J = 2	J = 3	J = 4	J = 5	J = 6
1	-4.1927-01	4.5818+00	3.0028+00	6.6668-02	3.5288-10	-2.8740-10
2	-5.7764-01	7.9650-01	2.5772+00	-4.3215-02	-2.2555-10	5.0932-11
3	-3.6964-01	9.8472-01	1.3532+00	-3.9579-02	1.2179-07	1.5543-07
4	-1.3708-01	1.0451+00	8.5761-01	-6.5037-02	2.0201-07	-1.0532-08
5	-1.6007-10	-9.8225-10	1.3097-09	2.2919-10	-4.1044-01	5.2599-01
6	-1.7542-08	3.9465-08	2.1337-07	-3.4308-08	-2.8911-01	-5.2007-02
	J = 1	J = 2	J = 3	J = 4	J = 5	J = 6
1	4.3072+00	1.9812+00	5.5273-01	1.0443+00	6.3346-10	-2.7649-10
2	5.7690-01	1.9017+00	2.7920-01	1.8218-01	-1.0868-10	4.9477-10
3	6.8754-01	1.0568+00	4.8556-01	1.6299-01	1.0489-07	-2.7985-07
4	1.8209+00	5.8193-01	2.9988-01	3.1823-01	-1.1016-07	-4.8300-07
5	1.5643-09	-2.3283-10	1.7462-10	5.0022-11	5.8332-01	7.9272-01
6	6.4232-08	1.2605-07	1.5987-07	-6.5515-08	7.6340-03	5.5089-01

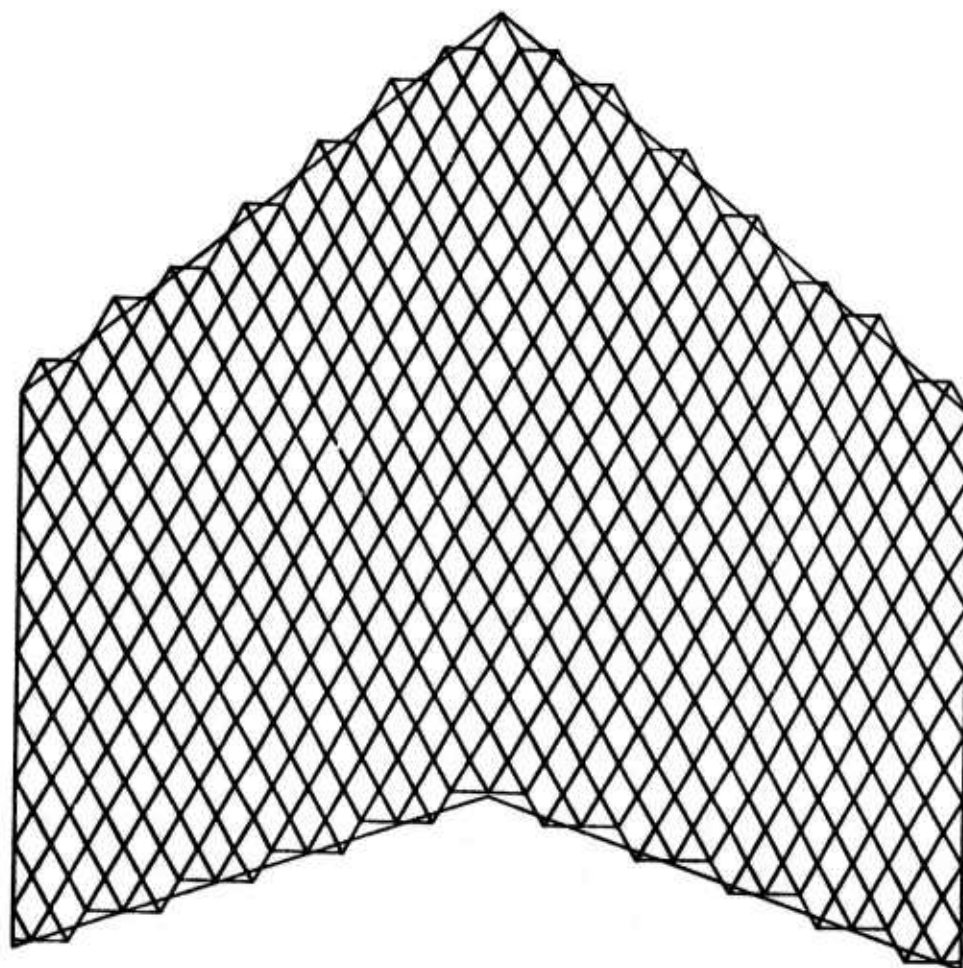


Fig. 16 - Mesh Used for Tapered Sweptback  $A = 1.45$ ,  $M = 2.0$



Table 33

TAPERED SHEET PILE BACK ANALYSIS; MOD=5; DELTA=1/13; MODES= 1, 2, 3, 4, 5, 6, 7, 8, 9, 10, 11, 12, 13, 14, 15, 16, 17, 18, 19, 20, 21, 22, 23, 24, 25, 26, 27, 28, 29, 30, 31, 32, 33, 34, 35, 36, 37, 38, 39, 40, 41, 42, 43, 44, 45, 46, 47, 48, 49, 50, 51, 52, 53, 54, 55, 56, 57, 58, 59, 60, 61, 62, 63, 64, 65, 66, 67, 68, 69, 70, 71, 72, 73, 74, 75, 76, 77, 78, 79, 80, 81, 82, 83, 84, 85, 86, 87, 88, 89, 90, 91, 92, 93, 94, 95, 96, 97, 98, 99, 100

	J = 1	J = 2	J = 3	J = 4	J = 5	J = 6
1	1.6736e02	2.5536e00	1.1980e00	-9.8694e03	-1.5887e05	-5.9574e05
2	-2.2986e03	4.9454e01	1.3359e00	-1.2129e02	-1.0664e05	-3.8366e05
3	-3.9239e03	5.3130e01	7.4084e01	-1.1789e02	-7.4387e06	-2.6130e05
4	1.6105e02	6.6318e01	4.2077e01	-1.2568e02	-8.1127e10	5.4888e08
5	2.4829e10	-4.7221e09	-2.3647e08	1.7208e09	-2.0613e02	5.1452e01
6	-3.6671e09	-7.2154e08	2.1170e07	-3.6334e09	-1.9631e02	9.7200e02

	J = 1	J = 2	J = 3	J = 4	J = 5	J = 6
1	2.6209e00	5.3358e01	9.9642e01	6.1701e01	-7.0886e05	1.1390e04
2	5.2637e01	6.8330e01	5.8888e01	1.5272e01	-4.5960e05	7.5305e05
3	5.5544e01	3.9887e01	4.6355e01	1.0732e01	-3.1458e05	5.2048e05
4	6.8988e01	1.6991e01	3.9086e01	2.4475e01	4.3724e08	-7.3327e02
5	-9.4115e09	-1.2631e08	-2.7547e08	3.8127e11	5.2707e01	3.2627e01
6	-6.8371e08	1.2227e07	8.9582e08	-6.2525e08	1.0436e01	3.7426e01

Table 34

TAPERED SWEPT BACK A=1.45, M=2., K=1., DELTA=1/13, MODES= 1, X, XOX, YOY, Y, XY

	J = 1	J = 2	J = 3	J = 4	J = 5	J = 6
1	6.0539-02	2.3386+00	1.3132+00	-3.7420+02	-5.6197+05	-9.9959-06
2	-1.3561-02	3.9678-01	1.3779+00	-4.6493-02	-3.7548-05	-4.9539-06
3	-1.9194-02	4.5909-01	7.7237-01	-4.5190+02	-2.6109+05	-2.6708-06
4	3.2751-02	5.6924-01	4.7209-01	-4.8623-02	-7.7489-10	0.1924-08
5	1.8445-09	-2.0900-09	-2.6266-08	6.7339-09	-7.7988-02	4.9190-01
6	-1.2747-08	-7.7644-08	2.0320-07	-1.4010-08	-7.4456-02	8.9965-02

87

	J = 1	J = 2	J = 3	J = 4	J = 5	J = 6
1	2.5951+00	6.0659-01	9.4311-01	6.2338-01	-4.9993-05	9.1672-05
2	5.1457-01	7.3036-01	4.6737-01	1.6030-01	-3.1678-05	0.0020-05
3	5.4791-01	4.2690-01	4.3814-01	1.1513-01	-2.1375-05	4.1209-05
4	6.6862-01	2.0534-01	3.6483-01	2.5209-01	4.9947-08	-8.7792-08
5	-5.8972-09	-1.5192-08	-2.4855-08	-4.9204-10	5.4217-01	3.2868-01
6	-6.5482-08	1.2420-07	9.1954-08	-6.1015-08	1.1878-01	2.7481-01

## REFERENCES

1. Garrick, I.E., and S.I. Rubinow, "Theoretical Study of Air Forces on an Oscillating or Steady Thin Wing in a Supersonic Main Stream," NACA Report 872 (1947).
2. Pines, S., J. Dugundji, and J. Neuringer, "Aerodynamic Flutter Derivatives for a Flexible Wing with Supersonic and Subsonic Edges," J. Aeronaut. Sci., 22:693-700 (1955).
3. Zartarian, G., and P. T. Hsu, "Theoretical Studies on the Prediction of Unsteady Supersonic Airloads on Elastic Wings," TR-56-97, Parts I and II, Wright Air Development Center, Wright-Patterson Air Force Base, Ohio, 1955.
4. Moore, M. T., and L. T. Andrew, "Unsteady Aerodynamics for Advanced Configurations, Part IV, Application of Supersonic Mach Box Method to Interesting Planar Lifting Surfaces," FDL-TDR-64-152, Wright-Patterson AFB, Ohio, May 1965.
5. Olsen, J. J., "Demonstration of a Supersonic Box Method for Unsteady Aerodynamics of Non-Planar Wings," FDL-TR-67-104, Parts I and II, AFFDL, Wright-Patterson AFB, Ohio, February 1969.
6. Woodcock, D. L., "A Comparison of Methods Used in Lifting Surface Theory," AGARD Report No. 583, Supplement to the Manual on Aeroelasticity, Part VI, 1971.
7. Appa, K., and G. C. C. Smith, "Further Development in Consistent Unsteady Supersonic Aerodynamic Coefficients," J. Aircraft, Vol. 9, No. 2, 1972.
8. Watkins, C. E., and J. H. Berman, "On the Kernel Function of the Integral Equations Relating Lift and Downwash Distributions of Oscillating Wings in Supersonic Flow," NACA Report 1257 (1956).
9. Cunningham, H. J., "Improved Numerical Procedure for Harmonically Deforming Lifting Surfaces from the Supersonic Kernel Function Method," AIAA J., Vol. 4, No. 11, November 1966.
10. Curtis, A. R., and R. W. Lingard, Jr., "Unsteady Aerodynamic Distributions for Harmonically Deforming Wings in Supersonic Flow," AIAA Paper 68-74, January 1968.

11. Harris, G. Z., "The Calculation of Generalized Forces on Oscillating Wings in Supersonic Flow by Lifting Surface Theory," ARC R&M 3453 (1965).
12. Cunningham, A.M., Jr., "Oscillatory Supersonic Kernel Function Method for Isolated Wings," J. Aircraft, Vol. 11, No. 10, October 1974.
13. Doggett, R. V., Jr., and R. L. Harder, "Subsonic Flutter Analysis Addition to NASTRAN," NASTRAN: User's Experiences, NASA TM X-2893, 1973, pp. 507-529.
14. Harder, R. L., R. H. MacNeal and W. P. Rodden, "A Study of Finite Element Method to Calculate Oscillatory Supersonic Lift Distributions Using the Acceleration Potential Kernel," NASA CR-111998 (1972).
15. Woodward, F. A., "Analysis and Design of Wing-Body Combinations at Subsonic and Supersonic Speeds," J. Aircraft, Vol. 5, No. 6, November-December 1968.
16. Brock, B. J., and J. A. Griffin, Jr., "The Supersonic Doublet-Lattice Method - A Comparison of Two Approaches," AIAA Paper 75-760, May 1975.
17. Jones, W. P., "Supersonic Theory for Oscillating Wings of Any Planform," ARC R&M 2655 (1953).
18. Allen, D. J., and D. S. Sadler, "Oscillatory Aerodynamic Forces in Linearized Supersonic Flow for Arbitrary Frequencies, Planforms and Mach Numbers," ARC R&M 3415 (1963).
19. Woodcock, D. L., Unpublished work at RAE, 1968.
20. Appa, K., and W. P. Jones, "Integrated Potential Formulation of Unsteady Aerodynamics for Interacting Wings," AIAA Paper 75-762, May 1975.
21. Giesing, J. P., and T. Kalman, "Oscillatory Supersonic Lifting Surface Theory Using a Finite Element Doublet Representation," AIAA Paper 75-761, May 1975.
22. Chen, L-T., E. O. Suci and L. Morino, "A Finite Element Method for Potential Aerodynamics Around Complex Configurations," AIAA Paper 74-107, January-February 1974.
23. Watkins, C. E., "Three-Dimensional Supersonic Theory," AGARD Manual on Aeroelasticity, Part II, Chapter 5, 1960, p. 49.
24. Miles, J. W., The Potential Theory of Unsteady Supersonic Flow, Cambridge University Press, 1959, p. 51.

25. Liepmann, H. W., and A. Roshko, Elements of Gasdynamics, John Wiley & Sons, New York, 1957, p. 390.
26. Cunningham, H. J., "Application of a Supersonic Kernel Function Procedure to Flutter Analysis of Thin Lifting Surfaces," NASA TN D-6012 (1970).
27. Harder, R. L., and W. P. Rodden, "Kernel Function for Nonplanar Oscillating Surfaces in Supersonic Flow," J. Aircraft, Vol. 8, No. 8, August 1971.
28. Young, V. Y. C., "A New Finite Element Supersonic Kernel Function Method in Lifting Surface Theory: User's Manual," LMSC-HREC TR D496668, Lockheed Missiles & Space Company, Huntsville, Ala., December 1975.
29. Fenain, M., and D. Guiraud-Vallee, "Numerical Calculation of Wings in Steady or Unsteady Supersonic Flow," Part 1: Steady Flow. Part 2: Unsteady Flow, Recherche Aerospatiale No. 115, 1966-67.
30. Stark, V. J. E., "Calculation of Aerodynamic Forces on Two Oscillating Finite Wings at Low Supersonic Mach Numbers," SAAB TN 53 (1964).

**SUPPLEMENTARY**

**INFORMATION**

ERRATA SHEET

AFFDL-TR-76-3, Volumes I and ~~II~~

AD-B 011 996L

1. Vol. I, Page 35, Last Paragraph, Sentence 1: Add asterisk to the end of the sentence.

2. Vol. I, Page 35, Bottom of Page, Add the following:  
\*After the completion of this work, Mr. Herbert J. Cunningham of NASA-Langley traced the discrepancy to a sign error in A. M. Cunningham's paper. After correction, the two versions agree to four decimal places. The tabulated results contained herein have been revised based on A. M. Cunningham's corrected version.

3. Vol. I, Pages:	52	Substitute Tables:	7
	53		8
	54		9
	57		11
	58		12
	59		13
	62		15
	63		16
	66		18
	67		19
	70		21
	71		22
	74		24
	75		25
	78		27
	79		28
	82		30
	83		31
	86		33
	87		34

~~4. Vol. II, Substitute Pages 45 and 46.~~

TABLE 7

RECTANGULAR ARZ.,  $M=1.2$ ,  $K=0.3$ ,  $\Delta E/\Delta X=0.75$ , MODES 1, 2, 3, 4, 5, 6, 7, 8, 9, 10, 11, 12, 13, 14, 15, 16, 17, 18, 19, 20, 21, 22, 23, 24, 25, 26, 27, 28, 29, 30, 31, 32, 33, 34, 35, 36, 37, 38, 39, 40, 41, 42, 43, 44, 45, 46, 47, 48, 49, 50, 51, 52, 53, 54, 55, 56, 57, 58, 59, 60, 61, 62, 63, 64, 65, 66, 67, 68, 69, 70, 71, 72, 73, 74, 75, 76, 77, 78, 79, 80, 81, 82, 83, 84, 85, 86, 87, 88, 89, 90, 91, 92, 93, 94, 95, 96, 97, 98, 99, 100, 101, 102, 103, 104, 105, 106, 107, 108, 109, 110, 111, 112, 113, 114, 115, 116, 117, 118, 119, 120, 121, 122, 123, 124, 125, 126, 127, 128, 129, 130, 131, 132, 133, 134, 135, 136, 137, 138, 139, 140, 141, 142, 143, 144, 145, 146, 147, 148, 149, 150, 151, 152, 153, 154, 155, 156, 157, 158, 159, 160, 161, 162, 163, 164, 165, 166, 167, 168, 169, 170, 171, 172, 173, 174, 175, 176, 177, 178, 179, 180, 181, 182, 183, 184, 185, 186, 187, 188, 189, 190, 191, 192, 193, 194, 195, 196, 197, 198, 199, 200, 201, 202, 203, 204, 205, 206, 207, 208, 209, 210, 211, 212, 213, 214, 215, 216, 217, 218, 219, 220, 221, 222, 223, 224, 225, 226, 227, 228, 229, 230, 231, 232, 233, 234, 235, 236, 237, 238, 239, 240, 241, 242, 243, 244, 245, 246, 247, 248, 249, 250, 251, 252, 253, 254, 255, 256, 257, 258, 259, 260, 261, 262, 263, 264, 265, 266, 267, 268, 269, 270, 271, 272, 273, 274, 275, 276, 277, 278, 279, 280, 281, 282, 283, 284, 285, 286, 287, 288, 289, 290, 291, 292, 293, 294, 295, 296, 297, 298, 299, 300, 301, 302, 303, 304, 305, 306, 307, 308, 309, 310, 311, 312, 313, 314, 315, 316, 317, 318, 319, 320, 321, 322, 323, 324, 325, 326, 327, 328, 329, 330, 331, 332, 333, 334, 335, 336, 337, 338, 339, 340, 341, 342, 343, 344, 345, 346, 347, 348, 349, 350, 351, 352, 353, 354, 355, 356, 357, 358, 359, 360, 361, 362, 363, 364, 365, 366, 367, 368, 369, 370, 371, 372, 373, 374, 375, 376, 377, 378, 379, 380, 381, 382, 383, 384, 385, 386, 387, 388, 389, 390, 391, 392, 393, 394, 395, 396, 397, 398, 399, 400, 401, 402, 403, 404, 405, 406, 407, 408, 409, 410, 411, 412, 413, 414, 415, 416, 417, 418, 419, 420, 421, 422, 423, 424, 425, 426, 427, 428, 429, 430, 431, 432, 433, 434, 435, 436, 437, 438, 439, 440, 441, 442, 443, 444, 445, 446, 447, 448, 449, 450, 451, 452, 453, 454, 455, 456, 457, 458, 459, 460, 461, 462, 463, 464, 465, 466, 467, 468, 469, 470, 471, 472, 473, 474, 475, 476, 477, 478, 479, 480, 481, 482, 483, 484, 485, 486, 487, 488, 489, 490, 491, 492, 493, 494, 495, 496, 497, 498, 499, 500, 501, 502, 503, 504, 505, 506, 507, 508, 509, 510, 511, 512, 513, 514, 515, 516, 517, 518, 519, 520, 521, 522, 523, 524, 525, 526, 527, 528, 529, 530, 531, 532, 533, 534, 535, 536, 537, 538, 539, 540, 541, 542, 543, 544, 545, 546, 547, 548, 549, 550, 551, 552, 553, 554, 555, 556, 557, 558, 559, 560, 561, 562, 563, 564, 565, 566, 567, 568, 569, 570, 571, 572, 573, 574, 575, 576, 577, 578, 579, 580, 581, 582, 583, 584, 585, 586, 587, 588, 589, 590, 591, 592, 593, 594, 595, 596, 597, 598, 599, 600, 601, 602, 603, 604, 605, 606, 607, 608, 609, 610, 611, 612, 613, 614, 615, 616, 617, 618, 619, 620, 621, 622, 623, 624, 625, 626, 627, 628, 629, 630, 631, 632, 633, 634, 635, 636, 637, 638, 639, 640, 641, 642, 643, 644, 645, 646, 647, 648, 649, 650, 651, 652, 653, 654, 655, 656, 657, 658, 659, 660, 661, 662, 663, 664, 665, 666, 667, 668, 669, 670, 671, 672, 673, 674, 675, 676, 677, 678, 679, 680, 681, 682, 683, 684, 685, 686, 687, 688, 689, 690, 691, 692, 693, 694, 695, 696, 697, 698, 699, 700, 701, 702, 703, 704, 705, 706, 707, 708, 709, 710, 711, 712, 713, 714, 715, 716, 717, 718, 719, 720, 721, 722, 723, 724, 725, 726, 727, 728, 729, 730, 731, 732, 733, 734, 735, 736, 737, 738, 739, 740, 741, 742, 743, 744, 745, 746, 747, 748, 749, 750, 751, 752, 753, 754, 755, 756, 757, 758, 759, 760, 761, 762, 763, 764, 765, 766, 767, 768, 769, 770, 771, 772, 773, 774, 775, 776, 777, 778, 779, 780, 781, 782, 783, 784, 785, 786, 787, 788, 789, 790, 791, 792, 793, 794, 795, 796, 797, 798, 799, 800, 801, 802, 803, 804, 805, 806, 807, 808, 809, 810, 811, 812, 813, 814, 815, 816, 817, 818, 819, 820, 821, 822, 823, 824, 825, 826, 827, 828, 829, 830, 831, 832, 833, 834, 835, 836, 837, 838, 839, 840, 841, 842, 843, 844, 845, 846, 847, 848, 849, 850, 851, 852, 853, 854, 855, 856, 857, 858, 859, 860, 861, 862, 863, 864, 865, 866, 867, 868, 869, 870, 871, 872, 873, 874, 875, 876, 877, 878, 879, 880, 881, 882, 883, 884, 885, 886, 887, 888, 889, 890, 891, 892, 893, 894, 895, 896, 897, 898, 899, 900, 901, 902, 903, 904, 905, 906, 907, 908, 909, 910, 911, 912, 913, 914, 915, 916, 917, 918, 919, 920, 921, 922, 923, 924, 925, 926, 927, 928, 929, 930, 931, 932, 933, 934, 935, 936, 937, 938, 939, 940, 941, 942, 943, 944, 945, 946, 947, 948, 949, 950, 951, 952, 953, 954, 955, 956, 957, 958, 959, 960, 961, 962, 963, 964, 965, 966, 967, 968, 969, 970, 971, 972, 973, 974, 975, 976, 977, 978, 979, 980, 981, 982, 983, 984, 985, 986, 987, 988, 989, 990, 991, 992, 993, 994, 995, 996, 997, 998, 999, 1000.

J = 1

	J = 1	J = 2	J = 3	J = 4	J = 5	J = 6	J = 7
1	2.1945-01	3.4793+00	3.6673-01	4.6102-02	7.5471-02	-3.6380-12	-4.1473-10
2	1.3913-02	-4.2706-01	1.0133+00	2.7655-03	2.5217-01	3.6380-12	1.8190-11
3	1.2334-02	2.9148-01	5.3292-03	3.0521-03	-1.3204-02	8.5111-09	2.0114-07
4	4.1291-02	7.9481-01	1.1476-01	1.3624-03	7.2717-02	1.9338-08	1.0223-06
5	2.6827-03	7.9295-02	-1.0735-02	3.0611-04	-1.3631-02	-2.9277-09	6.3823-07
6	8.1855-11	-1.9845-10	-4.0745-10	1.6257-11	-3.4925-10	-1.9810-02	4.0163-01
7	6.6984-10	-4.6439-08	3.2138-07	-1.7095-09	2.4989-07	-1.4321-02	-2.0093-01

52

J = 1

	J = 1	J = 2	J = 3	J = 4	J = 5	J = 6	J = 7
1	3.5314+00	-2.2655+00	1.3766+00	8.4363-01	3.5264+01	2.3041-10	1.2612+09
2	-4.3478+01	3.5386+01	-2.5576-01	1.3102+01	-4.4036+02	-2.8122-11	5.0206+10
3	2.4218+01	-1.3464+01	6.3809+02	8.2101-02	2.8725+02	2.0373+07	-3.8438-07
4	8.0513-01	-4.0356+01	2.8918-01	2.4168-01	4.2409+02	1.0283-06	-1.1114+08
5	7.4883-02	-3.5289+02	2.3446+02	3.5561-02	1.3617+02	6.3754+07	-5.0548+07
6	1.9340+09	-1.1581+09	2.4104+10	1.1217-10	-2.4253+11	3.4174+01	3.8667+01
7	-4.5866-08	1.5221+07	-1.3367+08	-1.0599-07	-3.1687-08	-2.0727-01	2.4200+01

TABLE 8

RECTANGULAR A=2, N=1, 2, K=6, DELTA=.075, MODES=1, 2, 3, 4, 5, 6, 7, 8, 9, 10, 11, 12, 13, 14, 15, 16, 17, 18, 19, 20, 21, 22, 23, 24, 25, 26, 27, 28, 29, 30, 31, 32, 33, 34, 35, 36, 37, 38, 39, 40, 41, 42, 43, 44, 45, 46, 47, 48, 49, 50, 51, 52, 53, 54, 55, 56, 57, 58, 59, 60, 61, 62, 63, 64, 65, 66, 67, 68, 69, 70, 71, 72, 73, 74, 75, 76, 77, 78, 79, 80, 81, 82, 83, 84, 85, 86, 87, 88, 89, 90, 91, 92, 93, 94, 95, 96, 97, 98, 99, 100, 101, 102, 103, 104, 105, 106, 107, 108, 109, 110, 111, 112, 113, 114, 115, 116, 117, 118, 119, 120, 121, 122, 123, 124, 125, 126, 127, 128, 129, 130, 131, 132, 133, 134, 135, 136, 137, 138, 139, 140, 141, 142, 143, 144, 145, 146, 147, 148, 149, 150, 151, 152, 153, 154, 155, 156, 157, 158, 159, 160, 161, 162, 163, 164, 165, 166, 167, 168, 169, 170, 171, 172, 173, 174, 175, 176, 177, 178, 179, 180, 181, 182, 183, 184, 185, 186, 187, 188, 189, 190, 191, 192, 193, 194, 195, 196, 197, 198, 199, 200, 201, 202, 203, 204, 205, 206, 207, 208, 209, 210, 211, 212, 213, 214, 215, 216, 217, 218, 219, 220, 221, 222, 223, 224, 225, 226, 227, 228, 229, 230, 231, 232, 233, 234, 235, 236, 237, 238, 239, 240, 241, 242, 243, 244, 245, 246, 247, 248, 249, 250, 251, 252, 253, 254, 255, 256, 257, 258, 259, 260, 261, 262, 263, 264, 265, 266, 267, 268, 269, 270, 271, 272, 273, 274, 275, 276, 277, 278, 279, 280, 281, 282, 283, 284, 285, 286, 287, 288, 289, 290, 291, 292, 293, 294, 295, 296, 297, 298, 299, 300, 301, 302, 303, 304, 305, 306, 307, 308, 309, 310, 311, 312, 313, 314, 315, 316, 317, 318, 319, 320, 321, 322, 323, 324, 325, 326, 327, 328, 329, 330, 331, 332, 333, 334, 335, 336, 337, 338, 339, 340, 341, 342, 343, 344, 345, 346, 347, 348, 349, 350, 351, 352, 353, 354, 355, 356, 357, 358, 359, 360, 361, 362, 363, 364, 365, 366, 367, 368, 369, 370, 371, 372, 373, 374, 375, 376, 377, 378, 379, 380, 381, 382, 383, 384, 385, 386, 387, 388, 389, 390, 391, 392, 393, 394, 395, 396, 397, 398, 399, 400, 401, 402, 403, 404, 405, 406, 407, 408, 409, 410, 411, 412, 413, 414, 415, 416, 417, 418, 419, 420, 421, 422, 423, 424, 425, 426, 427, 428, 429, 430, 431, 432, 433, 434, 435, 436, 437, 438, 439, 440, 441, 442, 443, 444, 445, 446, 447, 448, 449, 450, 451, 452, 453, 454, 455, 456, 457, 458, 459, 460, 461, 462, 463, 464, 465, 466, 467, 468, 469, 470, 471, 472, 473, 474, 475, 476, 477, 478, 479, 480, 481, 482, 483, 484, 485, 486, 487, 488, 489, 490, 491, 492, 493, 494, 495, 496, 497, 498, 499, 500, 501, 502, 503, 504, 505, 506, 507, 508, 509, 510, 511, 512, 513, 514, 515, 516, 517, 518, 519, 520, 521, 522, 523, 524, 525, 526, 527, 528, 529, 530, 531, 532, 533, 534, 535, 536, 537, 538, 539, 540, 541, 542, 543, 544, 545, 546, 547, 548, 549, 550, 551, 552, 553, 554, 555, 556, 557, 558, 559, 560, 561, 562, 563, 564, 565, 566, 567, 568, 569, 570, 571, 572, 573, 574, 575, 576, 577, 578, 579, 580, 581, 582, 583, 584, 585, 586, 587, 588, 589, 590, 591, 592, 593, 594, 595, 596, 597, 598, 599, 600, 601, 602, 603, 604, 605, 606, 607, 608, 609, 610, 611, 612, 613, 614, 615, 616, 617, 618, 619, 620, 621, 622, 623, 624, 625, 626, 627, 628, 629, 630, 631, 632, 633, 634, 635, 636, 637, 638, 639, 640, 641, 642, 643, 644, 645, 646, 647, 648, 649, 650, 651, 652, 653, 654, 655, 656, 657, 658, 659, 660, 661, 662, 663, 664, 665, 666, 667, 668, 669, 670, 671, 672, 673, 674, 675, 676, 677, 678, 679, 680, 681, 682, 683, 684, 685, 686, 687, 688, 689, 690, 691, 692, 693, 694, 695, 696, 697, 698, 699, 700, 701, 702, 703, 704, 705, 706, 707, 708, 709, 710, 711, 712, 713, 714, 715, 716, 717, 718, 719, 720, 721, 722, 723, 724, 725, 726, 727, 728, 729, 730, 731, 732, 733, 734, 735, 736, 737, 738, 739, 740, 741, 742, 743, 744, 745, 746, 747, 748, 749, 750, 751, 752, 753, 754, 755, 756, 757, 758, 759, 760, 761, 762, 763, 764, 765, 766, 767, 768, 769, 770, 771, 772, 773, 774, 775, 776, 777, 778, 779, 780, 781, 782, 783, 784, 785, 786, 787, 788, 789, 790, 791, 792, 793, 794, 795, 796, 797, 798, 799, 800, 801, 802, 803, 804, 805, 806, 807, 808, 809, 810, 811, 812, 813, 814, 815, 816, 817, 818, 819, 820, 821, 822, 823, 824, 825, 826, 827, 828, 829, 830, 831, 832, 833, 834, 835, 836, 837, 838, 839, 840, 841, 842, 843, 844, 845, 846, 847, 848, 849, 850, 851, 852, 853, 854, 855, 856, 857, 858, 859, 860, 861, 862, 863, 864, 865, 866, 867, 868, 869, 870, 871, 872, 873, 874, 875, 876, 877, 878, 879, 880, 881, 882, 883, 884, 885, 886, 887, 888, 889, 890, 891, 892, 893, 894, 895, 896, 897, 898, 899, 900, 901, 902, 903, 904, 905, 906, 907, 908, 909, 910, 911, 912, 913, 914, 915, 916, 917, 918, 919, 920, 921, 922, 923, 924, 925, 926, 927, 928, 929, 930, 931, 932, 933, 934, 935, 936, 937, 938, 939, 940, 941, 942, 943, 944, 945, 946, 947, 948, 949, 950, 951, 952, 953, 954, 955, 956, 957, 958, 959, 960, 961, 962, 963, 964, 965, 966, 967, 968, 969, 970, 971, 972, 973, 974, 975, 976, 977, 978, 979, 980, 981, 982, 983, 984, 985, 986, 987, 988, 989, 990, 991, 992, 993, 994, 995, 996, 997, 998, 999, 1000.

	J = 1	J = 2	J = 3	J = 4	J = 5	J = 6	J = 7
1	5.8667-01	2.7219+00	8.0985-01	1.1814+01	1.8021+01	-3.6380-11	3.0741-10
2	-2.5090-02	-5.0694-01	1.0368+00	-7.3947-03	2.6035-01	-4.7294-11	1.8463-10
3	1.9271-02	2.4862-01	2.1561-02	5.2470+03	-7.7118+03	3.7609-08	1.9153+07
4	1.0312-01	6.4061-01	2.0482-01	-5.8793-03	8.4200-02	8.5471-08	9.9957-07
5	4.2606+03	6.9358-02	-6.5173+03	9.3658-05	-1.2630-02	1.3333+09	6.5299-07
6	8.3674-11	8.9494-10	-3.2014-10	-9.0949-12	4.8021-10	-8.4538-02	4.4985-01
7	-8.8457-09	-2.9217-08	2.9009-07	-1.0034-08	2.4305-07	-5.5181-02	-1.6068-01

53

	J = 1	J = 2	J = 3	J = 4	J = 5	J = 6	J = 7
1	2.8254+00	-1.2471+00	7.0994-01	6.8599-01	1.9447-01	5.4686+11	-4.3454-10
2	-5.6458-01	6.0050-01	-4.1168-01	-1.6049-01	-8.1526-02	1.0810-10	7.2740-11
3	2.4167-01	-4.1618-02	6.2090-03	7.0095-02	1.4485-02	2.5020-07	-3.7071-07
4	6.5959-01	-1.8801-01	1.4774-01	2.2054-01	1.7689-02	1.0239-04	-1.1248-04
5	6.8794-02	-1.5124-02	1.1399-02	3.3955-02	1.1374-02	6.5520+07	-5.4308-07
6	1.4522-09	-1.2127-09	3.4077-10	3.3954-10	2.1828-10	4.1059+01	3.4427-01
7	-2.6844-08	1.4552-07	-2.3768-09	-1.0155-07	-3.1353-08	-1.8422-01	2.7363+01

TABLE 9

RECTANGULAR ANZ., HW1.Z, KAL., DELTA=0.075, MODES 1, X, XOX, YOT, XOXOY, Y, XY

	J = 1	J = 2	J = 3	J = 4	J = 5	J = 6	J = 7
1	5.2752-01	2.2135+00	9.8319-01	7.9413-02	2.2739-01	1.3097-10	-1.01642-10
2	-3.2510-01	-3.4868-01	8.6316-01	-7.8213-02	2.2569-01	0.0000	-1.01642-10
3	-3.7442-02	2.7406-01	-2.2768-02	-6.4868-03	-1.4517-02	1.0768-07	1.5672-07
4	5.5031-02	5.4867-01	2.3458-01	-5.4190-02	7.8238-02	2.4548-07	9.2152-07
5	-7.4468-03	7.3030-02	-1.4287-02	-2.5835-03	-1.3271-02	4.5198-08	6.2609-07
6	3.3469-10	1.2660-09	1.7462-10	-1.2369-10	-1.6007-10	-2.2594-01	5.7600-01
7	3.1992-08	3.4925-09	2.4345-07	-1.6618-08	2.3162-07	-1.2916-01	-8.0028-02

54

	J = 1	J = 2	J = 3	J = 4	J = 5	J = 6	J = 7
1	2.1383+00	-1.5332+02	-5.6436+02	5.3756-01	1.7005-02	-5.8208-10	5.8208-11
2	-5.7535-01	8.0311-01	-5.1815-01	-1.6255-01	-1.0868-01	1.3824-10	-5.2387-10
3	2.3243-01	3.2727-02	-3.0615-02	6.7033-02	4.2846-03	1.8219-07	-3.6094-07
4	5.2614-01	6.6262-02	-1.0600-02	2.1064-01	-5.2999-03	9.7947-07	-1.1035-06
5	6.6684-02	1.0709-03	3.2037-03	3.4347-02	1.0208-02	6.4279-07	-5.6660-07
6	1.3388-09	8.7311-11	1.6371-10	-4.1837-11	-8.7311-11	4.8397-01	3.1003-01
7	5.9266-08	6.9471-08	9.9828-08	-7.9919-08	-9.8335-09	-1.3061-01	2.2312-01

TABLE 11

RECTANGULAR A-Z... M-Z... K-J. DELTA=0.033. MODES= 1. X. X-1. Y-Y. X2-Y2-Y. Y. XY

	J = 1	J = 2	J = 3	J = 4	J = 5	J = 6	J = 7
1	1.8378-02	1.9939+00	-2.5144-01	2.6961-03	-4.2175-02	-5.4570-12	-2.7649-10
2	2.8398-03	-4.5169-02	3.6743-01	4.5313-05	1.1830-01	-2.2737-12	-1.7462-10
3	1.4494-03	1.6972-01	-1.6281-02	1.3164-04	-4.6364-03	6.3621-09	1.8769-07
4	2.3792-03	5.1466-01	-3.4353-02	-9.1203-04	8.6442-03	2.1155-09	1.7460-07
5	9.8266-05	4.5008-02	-4.0064-03	-1.8640-04	-1.4919-03	2.3201-09	3.0698-07
6	-4.5475-12	6.5484-11	-7.3283-10	-3.1832-12	3.3469-10	6.9307-04	4.7151-01
7	5.1386-10	-3.2771-08	3.5540-07	-1.1376-09	1.7310-07	-5.8801-04	-4.7368-02

	J = 1	J = 2	J = 3	J = 4	J = 5	J = 6	J = 7
1	2.0106+00	-3.3300-01	5.2182+01	5.2597-01	1.2703+01	4.1534+10	1.4552+10
2	-4.2406-02	1.5194+01	3.0270+02	-3.5008-02	1.0170+03	-7.4279-11	4.2443+11
3	1.7106+01	-2.4416-02	5.2430+02	4.5847+02	1.3384+02	1.8821+07	-3.8594+07
4	5.1839-01	-4.4258-02	1.2171+01	2.2086+01	4.1301+02	1.7412+07	-1.8428-07
5	4.8285+02	3.1197+03	1.2873+02	2.0091-02	4.8854+03	3.0463+07	4.0007+07
6	8.4886+11	2.3041+10	2.2434+10	-5.0553+10	-8.4886+11	4.7453+01	-1.3218+02
7	-3.1093+08	1.7218+07	1.8249+08	4.4927+08	-1.2148+08	-4.7107+02	6.8818+02

TABLE 12

RECTANGULAR A=2.0 K=0.5 DELTA=0.033, MODES I, X, XOX, YOY, XOXOY, Y, XY

	J = 1	J = 2	J = 3	J = 4	J = 5	J = 6	J = 7
1	7.0853-02	1.9194+00	-2.0462-01	1.0147-02	-3.1401-02	-1.0914-11	1.0550-09
2	1.0470-02	-6.0215-02	3.7686-01	-2.7121-05	1.2013-01	-9.0949-12	5.6389-11
3	5.4440-03	1.6303-01	-1.2104-02	4.4413-04	-3.7602-03	2.5761-08	1.9280-07
4	8.8973-03	4.9825-01	-2.4024-02	-3.8388-03	1.1513-02	8.5856-09	1.7622-07
5	3.1330-04	4.3666-02	-3.1835-03	-7.6736-04	-1.3629-03	9.3059-09	3.1647-07
6	-3.2742-11	-5.9663-10	0.0000	1.8190-12	1.3097-10	2.2832-03	4.5864-01
7	5.9845-10	-4.1859-08	3.6029-07	-4.8685-09	1.7368-07	-2.5044-03	-4.8956-02

58

	J = 1	J = 2	J = 3	J = 4	J = 5	J = 6	J = 7
1	1.9847+00	-3.1112-01	5.0775-01	5.2023-01	1.2365-01	3.7896-10	-7.2760-11
2	-4.9978-02	1.5858-01	2.8949-02	-3.6784-02	1.3361-05	9.0949-11	-7.2760-11
3	1.6824-01	-2.1820-02	5.0740-02	4.5317-02	1.2993-02	1.8753-07	-3.8801-07
4	5.1289-01	-3.9235-02	1.1844-01	2.1956-01	4.0267-02	1.7438-07	-1.8509-07
5	4.4735-02	-2.5515-03	1.2497-02	2.0720-02	4.7638-03	3.0697-07	-4.0922-07
6	-1.2066-09	0.0000	1.8190-11	2.3041-10	-6.6696-11	4.7048-01	-9.2189-03
7	-3.7004-08	1.7944-07	9.1283-09	-4.5608-08	-1.3160-08	-4.7982-02	6.9901-02



TABLE 15

ARROWHEAD A=4., M=1.12, K=5, DELTA=.056, MODES= 1, X, X.X, Y.Y, Y, XY

	J = 1	J = 2	J = 3	J = 4	J = 5	J = 6
1	1.4583-01	2.0667+00	1.9843+00	3.3742-02	0.0000	5.8208-11
2	6.9646-02	7.0730-01	1.1184+00	1.8295-02	0.0000	-1.1642-10
3	4.4921-02	4.7331-01	6.6537-01	1.1668-02	-9.8662-09	2.5824-07
4	4.5502-02	4.5304-01	5.7889-01	9.6533-03	-3.8744-08	7.8476-07
5	2.9104-11	2.3283-10	2.3283-10	0.0000	3.6060-03	3.2290-01
6	5.8149-08	-1.2660-07	1.6356-08	8.7675-09	2.9861-03	1.9849-01

	J = 1	J = 2	J = 3	J = 4	J = 5	J = 6
1	1.9633+00	3.9267-01	-3.0219-01	4.3616-01	2.3283-10	5.8208-11
2	6.4932-01	2.6929-01	-1.3625-01	2.4113-01	-5.8208-11	1.1642-10
3	4.3673-01	1.4508-01	-6.5737-02	1.6380-01	2.6586-07	1.4229-07
4	4.2404-01	1.0147-01	-4.1821-02	1.6383-01	8.1502-07	4.4398-07
5	0.0000	5.8208-11	0.0000	1.7462-10	3.1590-01	2.1918-01
6	-1.4732-07	-2.2780-07	-2.2256-07	-1.2445-07	1.9354-01	1.4923-01

TABLE 16

ARROWHEAD A=4.0, M=1.12, K=1.0, DELTA=.056, MODES= 1, X, X0A, Y0Y, Y, XY

	J = 1	J = 2	J = 3	J = 4	J = 5	J = 6
1	2.6696+01	2.0022+00	1.7400+00	6.0976-02	0.0000	1.7462-10
2	1.2311-01	6.8652-01	9.8650-01	4.1725-02	0.0000	5.8208-11
3	8.4783-02	4.5851-01	5.8487-01	2.6239-02	-3.4677-08	2.4951-07
4	9.8924-02	4.3061-01	5.1501-01	2.2503-02	-1.3629-07	7.5059-07
5	5.8208-11	1.1642-10	0.0000	1.4552-11	1.0249-02	3.3187-01
6	1.5349-07	-1.7096-07	-2.5437-08	2.3792-08	8.9984-03	2.0465-01

63

	J = 1	J = 2	J = 3	J = 4	J = 5	J = 6
1	1.7457+00	5.5483-01	-3.9763-02	3.8558-01	2.3283-10	0.0000
2	5.5192-01	3.3723-01	2.2336-02	2.1345-01	5.8208-11	5.8208-11
3	3.7583-01	1.8534-01	3.6361-02	1.4627-01	2.7588-07	1.4607-07
4	3.6286-01	1.4170-01	3.6210-02	1.4950-01	8.5350-07	4.5830-07
5	0.0000	5.8208-11	5.8208-11	0.0000	3.0941-01	2.1426-01
6	-2.2288+07	-1.7727-07	-1.7510-07	-1.3586-07	1.8885-01	1.4571-01

TABLE 18

ARROWHEAD A=4., M=1.25, K=5, DELTA=.052083333, MODES= 1, X, XOX, YOY, Y, XY

	J = 1	J = 2	J = 3	J = 4	J = 5	J = 6
1	1.3234-01	1.8579+00	1.6829+00	1.8844-02	0.0000	8.7311-11
2	7.0534-02	6.9460-01	9.8555-01	1.1208-02	7.2760-12	-2.0373-10
3	4.7455-02	4.5919-01	6.0703-01	7.6421-03	-1.1278-08	2.3545-08
4	4.6609-02	4.2971-01	4.9953-01	6.4852-03	-6.6793-09	2.2739-07
5	-1.4552-11	5.8208-11	1.1642-10	0.0000	7.3021-03	2.9543-01
6	2.5699-08	6.3825-08	6.9616-08	2.2665-09	5.5173-03	1.8599-01

66

	J = 1	J = 2	J = 3	J = 4	J = 5	J = 6
1	1.8080+00	3.0889-01	5.3657-03	3.5094-01	2.0373-10	-5.8208-11
2	6.6255-01	2.0767-01	8.2569-03	2.0395-01	2.9104-11	8.7311-11
3	4.3758-01	1.1122-01	1.5233-02	1.4134-01	2.7328-08	3.4750-08
4	4.1342-01	6.1366-02	2.2680-02	1.3861-01	2.2611-07	1.7593-07
5	-1.7462-10	1.4552-11	-5.8208-11	-5.8208-11	2.8950-01	1.7427-01
6	6.2428-08	-6.8569-08	-1.3679-09	-7.1159-09	1.8153-01	1.2076-01

TABLE 19

ARROWHEAD A=4., M=1.25 , K=1., DELTA=.0520833333, MODES= 1, A, Kx, Yy, Y, Xy

	J = 1	J = 2	J = 3	J = 4	J = 5	J = 6
1	3.1908-01	1.7484+00	1.5645+00	5.8870-02	1.4552-11	2.9104-11
2	1.6078-01	6.4668-01	9.0852-01	3.4236-02	2.9104-11	-8.7311-11
3	1.0959-01	4.2832-01	5.5589-01	2.3186-02	-4.2011-08	2.1799-08
4	1.2080-01	3.9982-01	4.6376-01	2.0229-02	-2.6295-08	2.3431-07
5	0.0000	5.8208-11	-1.1059-09	1.4552-11	2.4288-02	3.0038-01
6	8.3586-08	3.7398-08	6.9267-08	7.7707-09	1.8435-02	1.8990-01

67

	J = 1	J = 2	J = 3	J = 4	J = 5	J = 6
1	1.5739+00	4.5064-01	5.1727-02	3.2353-01	-8.7311-11	5.8208-11
2	5.3890-01	2.8147-01	4.4727-02	1.8718-01	2.6193-10	2.0373-10
3	3.5727-01	1.5853-01	4.1865-02	1.2991-01	3.5943-08	3.4750-08
4	3.4030-01	1.0338-01	4.0671-02	1.2944-01	2.2972-07	1.7491-07
5	-4.0745-10	1.0186-10	-4.3656-11	-5.8208-11	2.7958-01	1.7226-01
6	3.2800-08	-5.1368-08	-1.1642-09	-9.5024-09	1.7427-01	1.1916-01

TABLE 21

ARROWHEAD A=9., M=1.5621, K=5, DELTA=0.5207, MODES= 1. X, XOX, YOY, Y, XY

	J = 1	J = 2	J = 3	J = 4	J = 5	J = 6
1	-0.2564-02	1.2799+00	1.0238+00	5.3207+03	0.7417-06	1.3680-03
2	2.5029+02	4.0706+01	6.1295+01	3.5035-03	-2.3726-06	-4.03106-04
3	1.0019+02	3.2115+01	3.0411+01	2.6322-03	6.4402-07	1.1425-04
4	1.4193+02	3.1106+01	3.1503+01	2.5030+03	1.1402-07	2.9400-05
5	1.5631+05	1.0267+03	-1.0076+03	7.5574+00	6.3606-03	2.4732-01
6	-4.1916+06	-5.0117+04	2.9930+04	-1.9745+00	4.6314+03	1.5701-01

	J = 1	J = 2	J = 3	J = 4	J = 5	J = 6
1	1.2795+00	3.4100+01	2.5204+01	2.5001+01	1.5720+03	-4.9803+04
2	4.0523+01	2.0624+01	1.5711+01	1.5290+01	-4.3216+04	1.3745+04
3	3.1960+01	1.1969+01	1.1327+01	1.0969+01	1.1955+04	-3.0154+05
4	3.1032+01	0.0401+02	9.9967+02	1.0935+01	2.9449+05	-0.5532+06
5	1.0337+03	-6.0702+04	2.2047+04	3.2396+05	2.4570+01	1.2517+01
6	-5.0306+04	1.6606+04	-6.0429+05	-0.0217+06	1.5651+01	0.9666+02

TABLE 22

AFROMHEAD A=9.1 M=1.5621. K=1. DELIAR.05207. MODES= I. X. XOX. Y=Y, I, XI

I	J = 1	J = 2	J = 3	J = 4	J = 5	J = 6
1	1.3736-01	1.2156+00	1.0318+00	2.0611-02	3.4923-05	1.5551-03
2	8.0371-02	4.5459-01	6.1589-01	1.3335-02	-9.4786-06	-4.2755-04
3	5.8785-02	2.9976-01	3.8670-01	9.8136-03	2.5763-06	1.1830-04
4	6.6285-02	2.9071-01	3.2008-01	9.4548-03	4.5530-07	2.9243-05
5	6.2357-05	1.8033-03	-1.0767-03	3.0184-07	2.3361-02	2.4519-01
6	-1.6724-05	-4.9490-04	2.9646-04	-7.9010-08	1.6978-02	1.5683-01
I	J = 1	J = 2	J = 3	J = 4	J = 5	J = 6
1	1.2090+00	3.7982-01	2.4044-01	2.4485-01	1.5712-03	-4.9773-04
2	4.4468-01	2.2753-01	1.5067-01	1.4961-01	-9.3193-04	1.3737-04
3	2.9226-01	1.3372-01	1.0900-01	1.0728-01	1.1949-04	-3.8132-05
4	2.8633-01	9.2015-02	9.5942-02	1.0733-01	2.9436-05	-8.5490-06
5	1.8314-03	-6.0675-04	2.1997-04	3.2387-05	2.3921-01	1.2626-01
6	-5.0243-04	1.6658-04	-4.0297-05	-8.8195-06	1.5178-01	9.0379-02

TABLE 24

ARROWHEAD A=4., M=2., K=5, DELTA=05, MODES= 1. X. XOX. Y=Y, V. XY

I	J = 1	J = 2	J = 3	J = 4	J = 5	J = 6
1	0.5894-02	1.2705+00	6.5434-01	7.7776-03	2.7285-12	-2.3283-10
2	3.1926-02	4.6270-01	5.3967-01	4.8743-03	-5.4570-12	1.3097-10
3	2.0556-02	3.0769-01	3.3271-01	3.4408-03	2.7558-10	-1.5149-08
4	1.7595-02	2.6628-01	2.7684-01	3.0193-03	8.4676-10	-4.5831-08
5	4.6384-11	2.9104-10	5.8208-11	4.5475-12	8.8484-03	2.4270-01
6	-1.0123-09	-1.0725-08	-1.0172-08	-3.9472-10	5.9020-03	1.5130-01

I	J = 1	J = 2	J = 3	J = 4	J = 5	J = 6
1	1.2745+00	1.6292-01	2.4030-01	2.4350-01	-1.7462-10	8.7311-11
2	4.6175-01	1.4162-01	1.3362-01	1.4683-01	-1.0186-10	-8.0036-11
3	3.0657-01	6.3855-02	4.8852-02	1.0424-01	-1.5702-08	-1.8516-08
4	2.8535-01	6.7384-02	8.5582-02	1.0481-01	-4.8875-08	-4.9484-08
5	5.5297-10	0.0000	-2.1828-11	-1.0186-10	2.4076-01	1.0222-01
6	-1.1045-08	-1.0987-09	-2.3210-09	7.4215-10	1.4971-01	7.4685-02

TABLE 25

ARROWHEAD A=9., M=2., K=1., DELTA=.05, MODES= 1, X, 1.X, Y, Y, Y, X, Y

	J = 1	J = 2	J = 3	J = 4	J = 5	J = 6
1	2.4399-01	1.1934+00	8.7873-01	3.0325-02	2.1828-11	0.0000
2	1.1678-01	4.3121-01	5.4979-01	1.8988-02	0.0000	7.2760-11
3	7.5300-02	2.8973-01	3.3941-01	1.3410-02	9.8225-10	-1.4974-08
4	6.5984-02	2.7399-01	2.8326-01	1.1827-02	2.9231-09	-4.5336-08
5	2.2555-10	-2.9104-11	-5.8208-11	9.0949-12	3.4218-02	2.4272-01
6	-2.4229-09	-1.0492-08	-9.9972-09	-1.3897-09	2.2788-02	1.5212-01

75

	J = 1	J = 2	J = 3	J = 4	J = 5	J = 6
1	1.2051+00	1.9342-01	2.2804-01	2.3909-01	-5.8208-11	0.0000
2	4.2521-01	1.5695-01	1.2747-01	1.4404-01	1.4552-11	-5.0932-11
3	2.8396-01	9.2743-02	9.2929-02	1.0232-01	-1.5993-08	-1.6473-08
4	2.6954-01	7.3189-02	8.3007-02	1.9317-01	-4.7490-08	-4.9644-08
5	8.7311-11	1.1842-10	9.4587-11	1.3097-10	2.3592-01	1.8290-01
6	-7.4942-09	-2.3792-09	-2.0300-09	1.0914-09	1.4581-01	7.5037-02

TABLE 27

TAPERED SWEPT BACK A=1.45, M=1.04, K=5, DELTA=104, MODES=1, X, XOX, Y=Y, Y, XY

	J = 1	J = 2	J = 3	J = 4	J = 5	J = 6
1	-1.3181-01	4.4124+00	3.3235+00	9.8230-02	1.3915-10	3.1287-10
2	-3.6692-01	3.3331-02	2.6914+00	-7.3766-02	-7.1850-11	-1.5280-10
3	-1.7282-01	7.2463-01	1.1227+00	-3.9702-02	-9.6288-09	1.4128-06
4	-4.7495-02	9.4609-01	9.5596-01	3.0814-03	-1.1802-07	1.3609-05
5	-4.3656-11	-1.1642-10	-1.0477-09	7.2760-12	-9.0066-02	9.6684-01
6	3.6414-07	-1.8669-06	2.6448-06	5.3173-08	-4.8242-02	-1.2109-01
7						
8						
9						
10						
11						
12						
13						
14						
15						
16						
17						
18						
19						
20						
21						
22						
23						
24						
25						
26						
27						
28						
29						
30						
31						
32						
33						
34						
35						
36						
37						
38						
39						
40						
41						
42						
43						
44						
45						
46						
47						
48						
49						
50						
51						
52						
53						
54						
55						
56						
57						
58						
59						
60						
61						
62						
63						
64						
65						
66						
67						
68						
69						
70						

TABLE 28

TAPERED SWEPT BACK A=1.45, M=1.04, K=1.0, DELTA=.104, MODES=1, X, XOX, YOY, Y, XY

	J = 1	J = 2	J = 3	J = 4	J = 5	J = 6
1	4.1151e-01	6.7422e-00	2.5092e-00	2.1706e-01	3.2014e-10	8.7311e-11
2	7.3971e-01	5.3903e-01	2.3181e-00	-1.1147e-01	2.9104e-11	0.0000
3	3.4284e-01	9.5109e-01	9.5867e-01	-5.5721e-02	-3.5798e-09	1.4807e-04
4	1.2597e-01	9.9910e-01	7.8181e-01	-1.0915e-02	-4.9107e-08	1.9441e-05
5	1.4552e-10	2.4738e-10	-1.1642e-09	1.4552e-11	-3.6341e-01	5.2204e-01
6	9.2207e-07	-2.4119e-04	3.0225e-04	1.1653e-07	-2.2784e-01	-1.3089e-01

	J = 1	J = 2	J = 3	J = 4	J = 5	J = 6
1	4.1340e+00	1.5799e+00	-1.4539e-01	1.2561e+00	7.8580e+10	-1.1642e-10
2	2.9260e-01	1.8187e+00	6.1542e-02	1.7288e-01	-2.4738e-10	0.0000
3	8.6857e-01	7.6609e-01	3.9324e-01	2.1238e-01	1.4015e-06	-6.1578e-07
4	9.0190e-01	4.9735e-01	1.0310e-01	3.7606e-01	1.3472e-05	-6.5963e-06
5	-2.1828e-10	-4.0745e-10	-9.3132e-10	1.2369e-10	5.7780e-01	6.8338e-01
6	-2.2070e-04	4.9401e-07	4.2171e-07	-1.1099e-06	-5.6445e-02	4.3131e-01

TABLE 30

TAPERED SWEPT BACK A=1.45, M=1.2, K=0.5, DELTA=1/15, MODES= 1, 2, 3, 4, 5, 6, 7, 8, 9, 10, 11, 12

	J = 1	J = 2	J = 3	J = 4	J = 5	J = 6
1	1.3565-01	3.5750+00	3.4803+00	1.1768-01	-9.0949-12	-8.3037-10
2	-1.8169-01	1.7002-01	2.7725+00	2.3604-02	-1.5643-10	-1.6189-10
3	-1.2875-01	5.9296-01	1.4206+00	9.4338-03	3.2313-08	1.4208-07
4	4.7044-03	8.3477-01	9.5303-01	3.5713-03	4.9700-08	-6.0027-08
5	-3.1650-10	6.9122-10	-6.4028-10	4.6384-11	-1.1739-01	4.5628-01
6	-2.6321-09	2.6845-08	2.0750-07	-6.8858-09	-9.9507-02	-7.1841-02

	J = 1	J = 2	J = 3	J = 4	J = 5	J = 6
1	3.3245+00	1.2092+00	-9.5865+01	9.3506-01	-4.6953-11	4.0018-10
2	-5.8277-02	2.1220+00	-1.1153+00	9.4636-02	-7.9353-11	2.1828-10
3	4.5065-01	1.2218+00	-4.5034+01	9.6532-02	1.3112-07	-2.7595-07
4	7.7877-01	4.5910-01	-1.0999+01	2.8323-01	-8.4787-08	-4.5565-07
5	4.2382-10	9.8953-10	8.7311-11	1.2278-10	4.5551-01	8.2452-01
6	2.4524-08	1.1237-07	9.0527-08	-7.5471-08	-6.5912-02	6.2944-01

TABLE 31

TAPERED SNEYD BACK A=1.15, M=1.2, K=1., DELTA=1/15, MODES= 1, X, X0, Y0, Y, XY

	J = 1	J = 2	J = 3	J = 4	J = 5	J = 6
1	-3.2607-01	3.9100+00	2.4705+00	4.1587+02	-2.5466-11	-4.1109-10
2	-7.4408-01	8.1954-01	1.9610+00	-1.2525-01	-7.2760-12	2.1100-10
3	-4.0428-01	9.6317-01	9.8004-01	-1.0005-01	9.4667-08	1.4383-07
4	-1.0930-01	9.0506-01	7.3264-01	-7.2763-02	1.2852-07	-2.9266-08
5	-4.2928-10	7.0941-10	1.3388+09	6.9122+11	-3.3514-01	5.8547-01
6	2.8740-09	1.9791-09	2.0595-07	-3.4375+08	-2.7134-01	2.8904-02

83

	J = 1	J = 2	J = 3	J = 4	J = 5	J = 6
1	3.4045+00	1.5363+00	6.2162-02	7.6921+01	5.5388-10	-1.4916-09
2	4.6647-01	1.6867+00	1.0430-02	8.2418-02	-1.4097-10	2.4738-10
3	8.3511-01	8.3535-01	3.8506-01	1.1009+01	1.0128-07	-2.4670-07
4	8.3642-01	4.6555-01	1.9308-01	2.7028-01	-1.1317-07	-4.0481-07
5	6.0390-10	1.0186-10	-7.2760-11	-3.2105-10	6.0941-01	6.8142-01
6	2.8955-08	9.4718-06	1.4772-07	-6.9727-08	6.6805-02	5.0812-01

TABLE 33

TAPERED SWEEP BACK A=1.45, M=2.0, K=5, DELTA=1/13, MODES= P, X, XOX, YOY, Y, XY

	J = 1	J = 2	J = 3	J = 4	J = 5	J = 6
1	8.8978-02	2.4743+00	1.2513+00	3.6333+03	1.8827-09	9.8862-10
2	2.7574-02	4.5286-01	1.3624+00	-5.6204+03	1.7802-09	8.4492-10
3	1.8770-02	5.0048-01	7.6032-01	-7.5210-03	1.7833-08	2.3495-07
4	2.8947-02	6.4166-01	4.3536-01	-7.9315+03	6.9613-09	8.6963-08
5	-3.5925-10	-4.5866-09	-2.3530-08	1.7480-09	-9.2156-03	5.0617-01
6	-1.4797-01	-7.5166-08	2.1094-07	-2.6494+09	-1.4452-02	9.2763-02

86

	J = 1	J = 2	J = 3	J = 4	J = 5	J = 6
1	2.5463+00	2.6970-01	1.0222+00	6.0545+01	4.5475-13	-1.8146-08
2	4.8096-01	5.6784-01	4.6494-01	1.4531-01	-1.3370-10	-1.7026-08
3	5.2178-01	3.0862-01	4.3617-01	1.0188+01	2.2007-07	-2.8302-07
4	6.6896-01	1.0060-01	3.9236-01	2.4075-01	8.5262-08	-1.3280-07
5	-7.1741-09	-1.1467-08	-2.6834-08	5.6616+10	5.1684-01	2.8179-01
6	-7.3873-08	1.1340-07	7.7867-08	-6.3500-08	9.7777-02	2.5391-01

TABLE 34

TAPERED SHEET BACK A=1.45, M=2., K=1., DELTA=1/13, MODES= 1, X, XOX, YOY, Y, KY

	J = 1	J = 2	J = 3	J = 4	J = 5	J = 6
1	2.3951-01	2.1120+00	1.4588+00	2.0294-03	8.0909-09	2.2756-09
2	4.0241-02	2.9270-01	1.4372+00	-3.0918-02	7.5597-09	1.4052-09
3	1.4732-02	3.8466-01	8.1388-01	-3.0299-02	7.9068-08	2.8207-07
4	7.6511-02	5.0956-01	5.1102-01	-3.5292-02	2.8806-08	9.8325-08
5	1.7790-09	1.1278-09	-2.8478-08	7.0540-09	-4.5986-02	4.6674-01
6	-1.5265-08	-7.8280-08	1.9476-07	-1.2315-08	-6.3733-02	7.8410-02
1	J = 1	J = 2	J = 3	J = 4	J = 5	J = 6
1	2.3415+04	4.9790-01	8.5531-01	5.8216-01	-1.3461-09	-1.9703-08
2	3.6613-01	7.0869-01	3.6326-01	1.3455-01	-2.8285-10	-1.8248-08
3	4.3985-01	4.1441-01	3.5988-01	9.6556-02	2.2630-07	-2.9923-07
4	5.9879-01	1.7936-01	3.3482-01	2.3796-01	8.2492-08	-1.3536-07
5	-2.9413-09	-1.6385-08	-2.1813-08	-3.5106-10	5.0627-01	2.9958-01
6	-7.4173-08	1.2177-07	7.6107-08	-6.3699-08	9.6434-02	2.6437-01